JANUARY 1979

FINAL TECHNICAL REPORT

A NESTED NUMERICAL TIDAL MODEL OF THE SOUTHERN NEW ENGLAND BIGHT

BY

ROBERT B. GORDON
GRADUATE RESEARCH ASSISTANT
AND
MALCOLM L. SPAULDING
ASSOCIATE PROFESSOR AND PRINCIPAL INVESTIGATOR

OCEAN ENGINEERING DEPARTMENT
UNIVERSITY OF RHODE ISLAND
KINGSTON, RHODE ISLAND 02881

SPONSORED BY

NATIONAL AERONAUTICS AND SPACE ADMINISTRATION
LANGLEY RESEARCH CENTER
HAMPTON, VIRGINIA 23665

GRANT NO.: NSG 1008

TITLE: DEVELOPMENT OF THREE-DIMENSIONAL NUMERICAL POLLUTANT TRANSPORT MODELING TECHNIQUES FOR CONTINENTAL SHELF APPLICATIONS

ABSTRACT

During earlier stages of this contract, efforts were focused on the development and application of a three-dimensional numerical model for predicting pollutant and sediment transport in estuarine and coastal environments. To successfully apply the pollutant and sediment transport model to Rhode Island coastal waters, it was determined that the flow field in this region had to be better described through the use of existing numerical circulation models.

As a first effort in this regard, a nested, barotropic numerical tidal model has been applied to the southern New England Bight (Long Island, Block Island, Rhode Island Sounds, Buzzards Bay, and the shelf south of Block Island). The numerical scheme employed is that of Greenberg (1977). This explicit finite difference scheme employs forward time and centered spatial differences with the bottom friction term being evaluated at both time levels. Horizontal friction and advective terms have been neglected.

Previous numerical studies of the tidal dynamics in this region were limited by inadequate information for the tide height boundary condition between Montauk Point, Block Island and Martha's Vineyard. Using existing tide records on the New England shelf, adequate information was available to specify the tide height boundary condition further out on the shelf. Preliminary results are generally within the accuracy of the National Ocean Survey (NOS) tide table data. Modeled co-range and co-tidal lines also agree with available data.

ACKNOWLEDGEMENTS

The authors are indebted to Jack Fancher, Elmo Long and Steacy Hicks (National Ocean Survey, N.O.A.A.); Robert Beardsley (Woods Hole Oceanographic Institution); Richard Callaway (U.S. E.P.A.); Wendell Brown (University of New Hampshire) and Harold Mofjeld (Pacific Marine Environmental Lab., N.O.A.A.) for furnishing data. David Greenberg (Environment Canada) kindly supplied a manuscript describing his numerical procedure which was employed in this study. Charles Beauchamp (University of Rhode Island) offered many useful suggestions and provided much information regarding the tides in the Southern New England Bight.

The computations were carried out at the University of Rhode Island Academic Computer Center (A.C.C.). We are grateful to the staff of the A.C.C. for their generous support in all aspects of the computational effort.

The study was funded in its entirety by the National Aeronautics and Space Administration, Marine and Applied Technology Office, Langley Research Center under Grant Number NSG 1008.

TABLE OF CONTENTS

LIST OF FIGURES

LIST OF FIGURES (CONT.)

LIST OF TABLES

CHAPTER I -- INTRODUCTION

During earlier stages of this research, efforts were focused on the development and application of a three-dimensional numerical model for predicting pollutant and sediment transport in estuarine and coastal environments (Hunter and Spaulding, 1975; Pavish and Spaulding, 1977). This numerical procedure was verified by running numerous test simulations for which analytical solutions were available. In addition, the model was used to predict the long term diffusion and advection of dilute neutrally and negatively buoyant suspended sediment clouds resulting from an instantaneous release of barged dredge spoil at Brown's Ledge in Rhode Island Sound, an area which is under consideration by the U.S. Army Corps of Engineers as a disposal site for dredged spoil material.

It was determined that the accuracy of such predictions would be seriously limited by the accuracy of the prescribed flow field. With this motivation, effort was undertaken to better describe and predict the flow field in the Rhode Island Sound region by use of existing numerical circulation models. As a first effort, a nested, barotropic numerical tidal model has been applied to the Southern New England Bight (Long Island, Block Island, Rhode Island Sounds, Buzzards Bay, and the Shelf south of Block Island). Figures I.1 and I.2 show the location of the Southern New England Bight and its component water bodies.

CHAPTER II -- REVIEW OF PREVIOUS OBSERVATIONS AND COMPUTATIONS IN THE SOUTHERN NEW ENGLAND BIGHT

II.1 Field Studies

Tides and currents in the southern New England Bight have been studied quite extensively. A brief summary of the studies is presented here. A more detailed description may be found in Beauchamp (1978).

Table II.1 presents a synopsis of the major observations of tides and currents in the southern New England Bight to date. A number of these studies have specifically addressed tides and tidal currents -- others have dealt with residual currents (Cook, 1966; Hollman and Sandberg, 1972; Pryterch, 1929; Larkin and Riley, 1967; Paskausky and Murphy, 1978) and wave induced flows in the bottom boundary layer (Griscom, 1977). These residual and wave induced current measurements are not of primary importance in the present numerical modeling effort but are listed in Table II.1 for completeness since future efforts to predict sediment and pollutant transport must address time scales longer and shorter than those of the tides.

The primary sources of data used in this study are the tide data compiled by N.O.A.A. National Ocean Survey (NOS, 1978) used for model verification and the tide data reported by Hicks (1968), Swanson (1976), Beardsley, et al (1977), Callaway (1977), Mofjeld (1977), NOS (1977) and Brown (1978) used to prescribe tide height boundary conditions.

In addition, a comprehensive study of tidal currents was performed by NOS in Long Island Sound in 1965 through 1967 (Long, 1978). Approximately 160 stations were occupied during

the course of that investigation, and harmonic constants have been determined for many of these stations. Beauchamp (1978) has made use of this data set for verification of his numerical modeling study.

II.2 Modeling Investigations

Early analytical studies were performed to investigate the resonant response of Long Island Sound (LeLacheur and Sammons, 1932; Redfield, 1950), tidal wave propagation in Long Island Sound (Redfield, 1950) and tidal interference phenomena in Vineyard and Nantucket Sounds (Redfield, 1953). More recently, Swanson (1971) has estimated the primary seiche period for Long Island Sound using the Defant Method (Defant, 1961).

A summary of numerical circulation models applied to regions within the southern New England Bight is given in Table II.2. A detailed description of these modeling investigations may be found in Beauchamp (1978). The most complete numerical investigation of tides and tidal currents is that of Beauchamp (1978). He employed Leendertse's multi-operational finite difference scheme for the entire southern New England Bight using 1.9 Km (1 N.M.) grid spacing. Model results were compared in detail with NOS tide data (NOS Tide Tables, 1978) and NOS tidal current data (Long, 1978).

II.3 Summary of the Tides and Tidal Currents of the Southern New England Bight

The primary circulation inducing mechanisms in the Southern New England Bight are the tides, wind and horizontal density variations. Although the predominant energetics are at tidal

frequencies, the wind and horizontal density variations may be important in driving the residual flow. The importance of wind and density induced circulation relative to the tidal flow varies depending on the specific location within the Bight. For example, it is well established (Paskausky and Murphy, 1976; Gordon and Pilbeam, 1975; Wilson, 1976) that Long Island Sound exhibits a two-layer density induced circulation. Also, Ianniello (1977) recently determined the importance of tidal non-linearties in inducing residual circulation in eastern Long Island Sound and Block Island Sound. Cook (1965) suggests that wind forcing is important in maintaining the residual flow in Rhode Island Sound. The present study, however, is solely concerned with tidal prediction, and wind and density variations will not be addressed.

The tides in the area range from semi-diurnal to mixed, mainly semi-diurnal. Defant's criterion (Defant, 1961) for determining the type of tide is:

$$R = \frac{K_1 + O_1}{M_2 + S_2}$$

where K_1 and O_1 are the principal diurnal harmonic constitutent amplitudes and M_2 and S_2 are important semi-diurnal harmonic constituent amplitudes. Swanson (1975) arbitrarily defines semi-diurnal tides as having values of R from 0 to 0.25 and mixed, mainly semi-diurnal as R from 0.25 to 1.5. Table III.1 shows the major tidal constituents for locations used as model boundary conditions. Also listed are the R values for each of these stations (refer to Fig. III.5 for location of these stations). It is seen that Woods Hole (located in Vineyard

Sound) is strongly mixed, mainly semi-diurnal while the shelf stations (MIT3, EPA2A, EPA2B, LT4, LT5, PICKET and KELVIN) have an average R of 0.26. Progressing into shallower waters, the tidal wave becomes much more strongly semi-diurnal as illustrated at Willets Point, located at the western end of Long Island Sound, which has an R of 0.12.

Propagation of the tidal wave in the study area may be observed from the co-range and co-tidal lines shown in Figs. II.3 through II.5. The tidal wave first enters Rhode Island Sound from the shelf between Block Island and Martha's Vineyard. It then proceeds radially across Rhode Island Sound to the mouths of Vineyard Sound, Buzzards Bay, and Narragansett Bay and to the eastern boundary of Block Island Sound. There is a slight amplification of the wave along the northern side of Rhode Island Sound due to decreasing depth. The wave then continues to progress up Buzzards Bay and Narragansett Bay where it is further amplified by shoaling and narrowing of these embayments. This same wave also progresses west to east through Vineyard Sound and is diminished due to interference with the progressing tidal wave entering Vineyard Sound from the Gulf of Maine (Redfield, 1953). The tide wave also progresses east to west into Block Island and Long Island Sounds. The progression of the tidal wave into Block Island Sound is relatively unimpeded through the Block Island - Rhode Island (north-south) transect relative to the shelf boundary between Montauk Point and Block Island (east-west transect). This is caused partially by the tidal interaction with Long Island Sound and partially due to the predominance of the east-west channel in the bathymetry of Block Island Sound.

The tidal wave is predominantly progressive on the shelf and in Rhode Island Sound. Tidal currents in these regions are rotary. The wave is relatively undistorted on the shelf except in the region just south of Nantucket (Nantucket Shoals). Western Block Island Sound and Long Island Sound exhibit strong standing wave characteristics. Redfield (1950) showed this region to be near resonance with the M_2 tidal period (12.42 hours) with a characteristic length of about one quarter of the tidal wavelength. Consequently, a velocity node and amplitude maximum exists in western Long Island Sound and a velocity maximum and amplitude node exists in eastern Long Island Sound near the Race. Studies of the resonant periods of Long Island Sound show a first mode at about 10 hours (Beauchamp, 1978).

Magnitudes of the tidal currents are roughtly 30 - 50 cm/s in Central Long Island Sound, 150 cm/s in the Race, 30 - 50 cm/s in Block Island Sound, 20 cm/s in Rhode Island Sound and 30 cm/s in Buzzards Bay.

The bathymetry of the area is illustrated in Figs. II.1 and II.2. Rhode Island Sound has a relatively smooth bottom with depths of around 55 m. where it meets the Southern New England Shelf and depths of 20 m. or less at its northern and western perimeter. Buzzards Bay also has a smooth bottom with maximum depths of 15 - 20 m. at its boundary with Rhode Island Sound and minimum depths of less than 8 m. at its eastern end.

Block Island Sound and the eastern part of Long Island Sound contain a more complex bathymetry characterized by steep bottom slopes. A channel of 35 m. or greater extends from

Rhode Island Sound through Block Island Sound reaching a maximum depth of over 100 m. in The Race. This channel then extends through Eastern Long Island Sound to Mattituck Sill. Mattituck Sill separates Eastern Long Island Sound from the broad, flat Central Basin. The Central Basin reaches depths of around 30 - 40 m. within 4 - 8 Km. of the Long Island shore. In the western portion of Long Island Sound, the bathymetry becomes more complex with depths less than 20 m.

CHAPTER III -- NUMERICAL SCHEME

III.1 Schematization

The nested finite difference grid system employed in this study is shown in Fig. III.4. As can be seen, two grids of differing grid spacing are meshed together. The larger grid is spaced at intervals of 5.6 km (3 N.M.), and the smaller grid is spaced at intervals of 1.9 km (1 N.M.). This grid spacing was chosen in order to obtain sufficient resolution to describe gradients in the dependent variables as well as bottom and planar topography while maintaining computational arrays small enough to allow easy computability. The smaller grid, which spans the southern New England Bight, is 158 x 28 in size. The larger grid is 38 x 20.

Concurrent with this study, Beauchamp (1978) was also modeling the tides in southern New England Bight with a 1.9 km (1 N.M.) grid spacing. He had difficulty in adequately specifying the surface elevation boundary condition along the large open boundaries extending from Montauk Point to Block Island and from Block Island to Martha's Vineyard (Fig. I.2). Variability in range and phase of the tidal wave along this boundary is seen in Figs. III.1 through III.3. It was decided that it would be desirable to extend this boundary further out onto the shelf where there existed less variability in the tide wave, hence the motivation for the nested grid procedure.

The bottom topography was represented by recording a representative depth value for each corner of the grid system. The depth data was obtained in digital format from N.O.A.A. Environmental Data and Information Service (Lawrence, 1977) when

available and from National Ocean Survey navigational charts otherwise. The configuration of the boundaries along the shoreline was drawn so as to maintain as closely as possible an equivalent surface area in the model. It should be noted that, because of a lack of information regarding the tide, the boundary between Martha's Vineyard and Nantucket Sound was taken as closed. The implications of this simplification are explored in Chapter IV - Results.

III.2 Finite Difference Equations

The vertically integrated equations of motion and continuity used in this study are:

x momentum

$$\frac{\partial u}{\partial t} - fv = - g \frac{\partial \xi}{\partial x} - \frac{\rho g \, u \, (u^2 + v^2)^{1/2}}{c^2 \, (h + \xi)} \qquad (1)$$

y momentum

$$\frac{\partial v}{\partial t} + fu = - g \frac{\partial \xi}{\partial y} - \frac{\rho g \, v (u^2 + v^2)^{1/2}}{c^2 \, (h + \xi)} \qquad (2)$$

continuity

$$\frac{\partial}{\partial x} \left[(h + \xi) \, u \right] + \frac{\partial}{\partial y} \left[(h + \xi) \, v \right] + \frac{\partial \xi}{\partial t} = 0 \qquad (3)$$

with a Cartesian Coordinate System being applied with the vertical axis positive in the upward direction. The vertical reference datum is taken as mean sea level. The following notation is employed:

t - time

x,y,z - a right handed Cartesian Coordinate System with z positive upwards

h - the depth of the undisturbed water

ξ - the elevation of the water surface

u,v - the depth averaged currents in the x and y directions, respectively.

$$u = \frac{1}{h + \xi} \int_{-h}^{\xi} \hat{u}(z)\, dz; \quad v = \frac{1}{h + \xi} \int_{-h}^{\xi} \hat{v}(z)\, dz$$

ρ - the density of the water

f - the Coriolis coefficient ($2\Omega \sin\phi$ where Ω is the angular velocity of the earth and ϕ is the latitude)

g - acceleration of gravity

c - Chezy bottom roughness coefficient related to the Manning coefficient (n) by:

$$C = \frac{H^{1/6}}{n} \quad \left[m^{1/2}/s\right]$$

It has been assumed that the water is of constant density and that direct tidal forcing is negligible. Wind stresses and the effects of variations in atmospheric pressure are not considered. The convective acceleration terms in Eqs. (2) and (3) have been assumed to be negligible (see Chapter V - Summary for further discussion of this approximation).

Equations (1) through (3) were put into the following finite difference form (Greenberg, 1977) using the grid notation illustrated in Fig. III.1:

$$\frac{\xi_{i,j}^{(t+\Delta t)} - \xi_{i,j}^{(t)}}{\Delta t} = -\frac{1}{\Delta x}\left[d_{i,j}^{(t)}\, u_{i,j}^{(t)} - d_{i-1,j}^{(t)}\, u_{i-1,j}^{(t)}\right] - \frac{1}{\Delta y}\left[e_{i,j-1}^{(t)}\, v_{i,j-1}^{(t)} - e_{i,j}^{(t)}\, v_{i,j}^{(t)}\right] \tag{4}$$

$$\frac{u_{i,j}^{(t+\Delta t)} - u_{i,j}^{(t)}}{\Delta t} = fr_{i,j}^{(t)} - g\left[\frac{\xi_{i+1,j}^{(t+\Delta t)} - \xi_{i,j}^{(t+\Delta t)}}{\Delta x}\right] - \frac{\rho g\, u_{i,j}^{(t+\Delta t)}\left[u_{i,j}^{2\,(t)} + r_{i,j}^{2\,(t)}\right]^{1/2}}{\left[\frac{1}{2}\left(C_{i,j} + C_{i+1,j}\right)\right]^2 d_{i,j}} \tag{5}$$

$$\frac{v_{i,j}^{(t+\Delta t)} - v_{i,j}^{(t)}}{\Delta t} = -fS_{i,j}^{(t+\Delta t)} - g\left[\frac{\xi_{i,j}^{(t+\Delta t)} - \xi_{i,j+1}^{(t+\Delta t)}}{\Delta y}\right] - \frac{\rho g\, v_{i,j}^{(t+\Delta t)}\left[S_{i,j}^{2\,(t)} + v_{i,j}^{2\,(t)}\right]^{1/2}}{\left[\frac{1}{2}\left(C_{i,j} + C_{i,j+1}\right)\right]^2 e_{i,j}} \tag{6}$$

where

$$d_{i,j} = \frac{1}{2}\left(h_{i,j} + \xi_{i,j} + h_{i+1,j} + \xi_{i+1,j}\right)$$

$$e_{i,j} = \frac{1}{2}\left(h_{i,j} + \xi_{i,j} + h_{i,j+1} + \xi_{i,j+1}\right)$$

$$r_{i,j} = \frac{1}{4}\left(v_{i,j-1} + v_{i+1,j-1} + v_{i,j} + v_{i+1,j}\right)$$

$$S_{i,j} = \frac{1}{4}\left(U_{i-1,j} + U_{i,j} + U_{i-1,j+1} + U_{i,j+1}\right)$$

The calculation procedure for surface elevation and horizontal velocity components is illustrated in Fig. III.2.

III.3 Nesting Procedure

In setting up the nested grid system for this study, the overlapping region was made to run along the x direction (Fig. III.4). The two grids are interactive; in other words, the dependent variables are solved in both grids at each time step, and an interpolation scheme is used so that the computations are "continuous" across the interface.

Figure III.3 shows the interface between the coarse and fine grids. Note that the points underlined are those dependent variables obtained by linear interpolation. Note also that, for the particular procedure employed, a 3 to 1 grid spacing ratio must be employed. Because the grid interface has been oriented in this x direction, only the y component of the horizontal velocity (v) and the surface elevation (ξ) must be interpolated. In order to insure conservation of volume in the overlap region, the interpolated velocities are adjusted in an iterative fashion so that the entire overlap strip obays conservation of mass. The procedure employed proved to be very stable numerically. Additional details can be obtained from Greenberg (1977).

III.4 Order of Computation

The sequence of computation is as follows:

1. ξ, u, v specified at $t = 0$ (initial conditions).
2. ξ along open boundaries is prescribed for $t + \Delta t$ (boundary conditions).
3. Calculate ξ on coarse grid from continuity equation at $t + \Delta t$.
4. Calculate ξ on fine grid from continuity equation at $t + \Delta t$.
5. Calculate u on coarse grid from x-momentum equation at $t + \Delta t$.
6. Calculate u on fine grid from x-momentum equation at $t + \Delta t$.
7. Calculate v on coarse grid from y-momentum equation at $t + \Delta t$.

8. Calculate v at edge of coarse grid using y-momentum equation and interpolating u and ξ at $t + \Delta t$.
9. Calculate v on fine grid from y-momentum equation at $t = \Delta t$.
10. Linearly interpolate v and ξ and iteratively adjust v to satisfy continuity of volume in the strip between the coarse and fine grid at $t + \Delta t$.
11. Increment time by Δt and proceed from step (2).

III.5 Initial Conditions

The model was operated from still water conditions, i.e. null velocities, and constant elevation. In some longer runs results from previous runs were used as initial conditions to speed convergence.

III.6 Boundary Conditions

Tidal elevations at the open boundaries of the model grid (see Fig. IV.1 for boundary locations) were specified using available tide data. Figure III.5 shows the locations for which tide data, in the form of harmonic constants, was available. (Stations are marked with an "x".) Table III.1 lists the amplitude and phase of the major constituents for these locations.

For the simulations discussed in Chapter IV, a mean tide boundary condition was employed. The mean tide was deduced by sampling the predicted tide at twelve intervals per tidal cycle and averaging a year's worth of these tidal cycles (Swanson, 1977). At all locations, a mean tidal period of 12.42 hours (M_2) exists. Figure III.6 illustrates the mean tidal curves used in specifying input boundary conditions.

In specifying the large shelf boundary conditions, it was found that shelf tide stations (LT-4, LT-5, EPA2, MIT3 and PICKET in Fig. III.5) were in phase and uniform in amplitude. Redfield (1953) notes, however, large changes in phase and amplitude in the vicinity of Nantucket Island. The model boundary condition in the vicinity of Nantucket was deduced from Redfield's (1953) co-range and co-tidal lines.

III.7 Time Increment

The restriction on the time increment Δt is that of Courant-Friedrich-Lewy:

$$\frac{\Delta x}{\Delta t} > 2\sqrt{2g\ H_{MAX}} \qquad (7)$$

Taking account of the maximum depth of water, H_{MAX}, encountered within the model, a value of $\Delta t = 47.06$ secs. was employed to insure that the numerical solution was fully stable at all times.

CHAPTER IV -- MODEL RESULTS

IV.1 Tide

Time histories at seven locations in the model grid were developed to observe the model performance during start up and to establish that a quasi-steady state had been reached. These locations are shown in Fig. IV.1, and the time histories are shown in Fig. IV.2. The initial transients are clearly seen, and these damp out in all locations by the third tidal cycle (step number 2280). High frequency oscillations due to seiching are seen in the transients at Newport (NPT) and Cape Cod Canal (CCC).

Comparison between the observed and computed tide are illustrated in Figs. IV.3 through IV.8. Figures IV.3, IV.4 and IV.5 show observed and computed co-range, high water interval and low water interval lines, respectively. Figures IV.6, IV.7 and IV.8 are a comparison of range, high water and low water intervals vs. distance along the x-axis of the 1.9 Km (1 N.M.) grid.

Agreement in range between observations and model results are uniformly good throughout the grid system with a mean difference of 0.09 m and a maximum difference of 0.27 m (in western Long Island Sound). Agreement in high water interval is not as uniform. Due to the poor resolution of topography in western Long Island Sound, the 16.5 hour line is computed to be too far east (refer to Fig. IV.4). In addition, high water occurs about 0.5 hours too early uniformly throughout Rhode Island Sound (refer to Fig. IV.7). The high water interval in the vicinity of Nantucket is off by approximately 1.5 hours. This

is due to a poor specification of the surface boundary condition in that region. Further refinement of this boundary condition should rectify this error. In addition, a tidal height specification should be specified in the region between Martha's Vineyard and Nantucket. Other regions in the model grid show better agreement. The mean difference in computed and observed high water interval is 0.29 hours with a maximum difference of 1.06 hours (in western Long Island Sound). Agreement in observed and computed low water interval is better than that for high water interval. The worst discrepancy occurs at the 10 hour line (see Fig. IV.5) in western Long Island Sound. The mean difference in computed and observed low water interval is 0.29 hours with a maximum difference of 0.76 hours (in western Long Island Sound). A comparison of observed (NOS tide stations) and computed tidal range and phase is summarized in Table IV.1.

IV.2 Velocity

Figures IV.9 through IV.14 show the velocity field at intervals of two lunar hours (12 lunar hours = 12.42 solar hours). A prominent feature is the high velocities in eastern Long Island Sound and western Block Island Sound (vicinity of The Race), near Montauk Point, in Vineyard Sound and just south of Nantucket (Nantucket Shoals). The tidal velocities in Rhode Island Sound are quite weak (of order 20-30 cm/s). Figures IV.12 and IV.14 illustrate the phasing difference between Long Island Sound and Buzzards Bay.

A comparison between observed and computed tidal currents has not been made; however, Beauchamp (1978) has made such comparison for a somewhat similar modeling effort.

CHAPTER V -- SUMMARY

The model results for tidal elevation were generally within the accuracy of NOS data. High and low water phasing were also within the accuracy of existing data with the exception of western Long Island Sound, the area in the immediate vicinity of Montauk Point and Nantucket Shoals.

Beauchamp's (1978) grid coincides with the small grid used in this study. The addition of the larger grid (to take advantage of existing shelf tide measurements) improved the description of the tide in southern New England Bight over that of Beauchamp. Specifically, range prediction in the vicinity of Montauk Point is improved by roughly 0.2 m, high water interval is improved by about 0.5 hours in Block Island Sound and low water interval is improved by about 0.5 hours in Rhode Island Sound. Also, a better representation of tidal phasing in western Long Island Sound is accomplished.

Western Long Island Sound is the region most poorly represented by the model. This may be attributed to the complex bathymetry and planar geometry of the region which is not adequately resolved by the 1.9 Km grid.

The non-linear convective acceleration terms were not included in the finite difference equations employed in this study since they are of second order importance. This can be concluded by comparison with Beauchamp's (1978) results which were obtained using Leendertse's multi-operational scheme for which the convective acceleration terms are retained. It should be noted, however, that although the convective acceleration terms are not of primary importance in describing tidal fluctuations,

they are of primary importance in determining tidally induced residual flow, especially in the vicinity of The Race.

The numerical procedure required 448K main storage on the University of Rhode Island's ITEL-5. Twenty minutes of central processor time was required to simulate one tidal cycle (950 time steps per tidal cycle).

This work constitutes a further refinement in supplying an accurate velocity field for use in the numerical transport models of Hunter and Spaulding (1975) and Pavish and Spaulding (1977) which were developed in an earlier stage of this contract.

REFERENCES

Beardsley, R.C., et al (1977), "Ocean Tides and Weather-Induced Bottom Pressure Fluctuations in the Middle Atlantic Bight", J. of Geophys. Rsch., 82(21), July 20, 1977.

Beauchamp, C.H. (1978), A Two-Dimensional Vertically Averaged Numerical Model of Tidal Dynamics in the Southern New England Intracoastal System, Masters Thesis, Ocean Engrg. Dept., Univ. of Rhode Island.

Beauchamp, C.H. and M.L. Spaulding (1978), "Tidal Circulation in Coastal Seas", Verification of Mathematical and Physical Models in Hydraulic Engineering -- Proceedings of the 26th Annual Hydraulics Division Specialty Conference, ASCE, pp. 518-528.

Bowman, Malcolm J. (1976), "The Tides of the East River, New York", J. of Geophys. Rsch., 81(9), March 20, 1976, pp. 1609-1616.

Brown, W., (1978), Personal Communication.

Callaway, R.J. (1977), Personal Communication.

Cook, G.S. (1966), "Non-Tidal Circulation in Rhode Island Sound", TM No. 369, Naval Underwater Research and Engrg. Station, Newport, R.I.

Defant, A. (1961), Physical Oceanography, Vol. 2, Pergamon Press, N.Y., 598 pp.

Gordon, Robert B. and Carol C. Pilbeam (1975), "Circulation in Central Long Island Sound", J. of Geophys. Rsch., 80(3), January 20, 1975, pp. 414-422.

Greenberg, D.A. (1977), "Mathematical Studies of Tidal Behaviour in the Bay of Fundy", Marine Sciences Directorate, Dept. of Fisheries and the Environment, Manuscript Report Series No. 46, 127 pp.

Griscom, C.A. (1978), Personal Communication.

Haight, F.J. (1936), "Currents in Narragansett Bay, Buzzards Bay, and Nantucket and Vineyard Sounds", Special Publication No. 208, U.S.C.&G.S.

Hicks, S.D., A.J. Goodheart, and C.W. Iseley (1965), "Observations of the Tide on the Atlantic Continental Shelf", J. of Geophys. Rsch., 70(8), April 15, 1965, pp. 1827-1830.

Hollman, R. and G.R. Sandberg (1972), "The Residual Drift in Eastern Long Island Sound and Block Island Sound", N.Y. Ocean Sci. Lab. Tech. Rpt. No. 15.

Hunter, David and Malcolm Spaulding (1975), Development of a Three Dimensional Numerical Water Quality Model for Continental Shelf Applications, Dept. of Ocean Engrg., Univ. of Rhode Island, Technical Report, 227 pp.

Ianniello, John P. (1977), "Tidally Induced Residual Currents in Estuaries of Constant Breadth and Depth", JMR, 35(4), 755-786.

Larkin, R.R. and C.A. Riley (1967), "A Drift Bottle Study in Long Island Sound", Bulletin of the Bingham Oceanographic Collection, 19, 62-71.

Lawrence, Lt.C. (1977), "Digital Bathymetry Data for the United States Coastal Regions, 34-35° North Latitude, Atlantic Coast", Key to Geophysical Record Documentation No. 8, DOC, NOAA, EDS, April 1977.

Mofjeld, H.O. (1977), Personal Communication.

NOS (1977), Personal Communication.

NOS (1978), Tide Tables for East Coast of North and South America, U.S. Dept. of Commerce, N.O.A.A., Rockville, Md.

Paskausky, David, F. and Donald L. Murphy (1976), "Seasonal Variation of Residual Drift in Long Island Sound", Estuarine and Coastal Marine Science, 4, 513-532.

Pavish, Danny and Malcolm Spaulding (1977), A Three-Dimensional Numerical Model for Predicting Pollutant and Sediment Transport Using an Eulerian-Lagrangian Marker Particle Technique, Dept. of Ocean Engrg., Univ. of Rhode Island, Technical Report, July 1977, 210 pp.

Pryterch, H.G. (1929), "Investigation of the Physical Conditions Controlling Spawning of Oysters and Occurrence, Distribution and Setting of Oyster Larvae in Milford Harbor, Connecticut", Bulletin of the U.S. Bureau of Fisheries, 44, 429-503.

Redfield, A.C. (1950), "The Analysis of Tidal Phenomena in Narrow Embayments", Pap. Phys. Oceanogr. Meteorgl., 11(4), pp. 1-36.

Redfield, Alfred C. (1953), "Interference Phenomena in the Tides of the Woods Hole Region", J. of Marine Rsch., 12(1), pp. 121-140.

Swanson, Craig and Malcolm Spaulding (1977), "Generation of Tidal Current and Height Charts for Narragansett Bay Using a Numerical Model", Dept. of Ocean Engrg., NOAA/Sea Grant, Univ. of Rhode Island Marine Tech. Rpt. 61, 10 pp.

Swanson, R.L. (1971), "Some Aspects of Currents in Long Island Sound", Ph.D. Thesis, Dept. of Oceanography, Univ. of Oregon.

Swanson, R.L. (1976), Tides, Mesa New York Bight Atlas Monograph 4, New York Sea Grant Institute, Albany, New York.

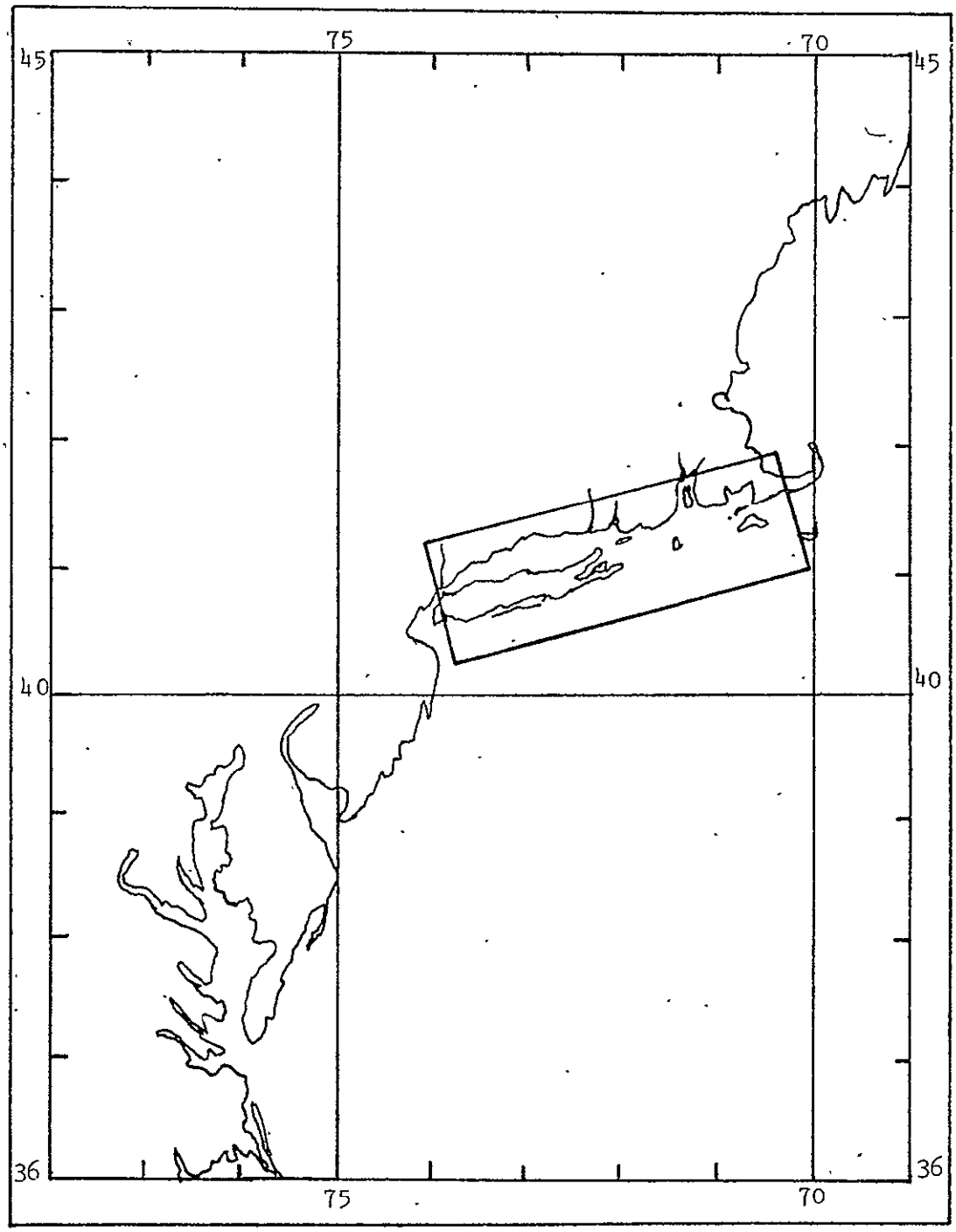

FIGURE I.1 LOCATION OF THE SOUTHERN NEW ENGLAND BIGHT ON THE EAST COAST OF THE UNITED STATES

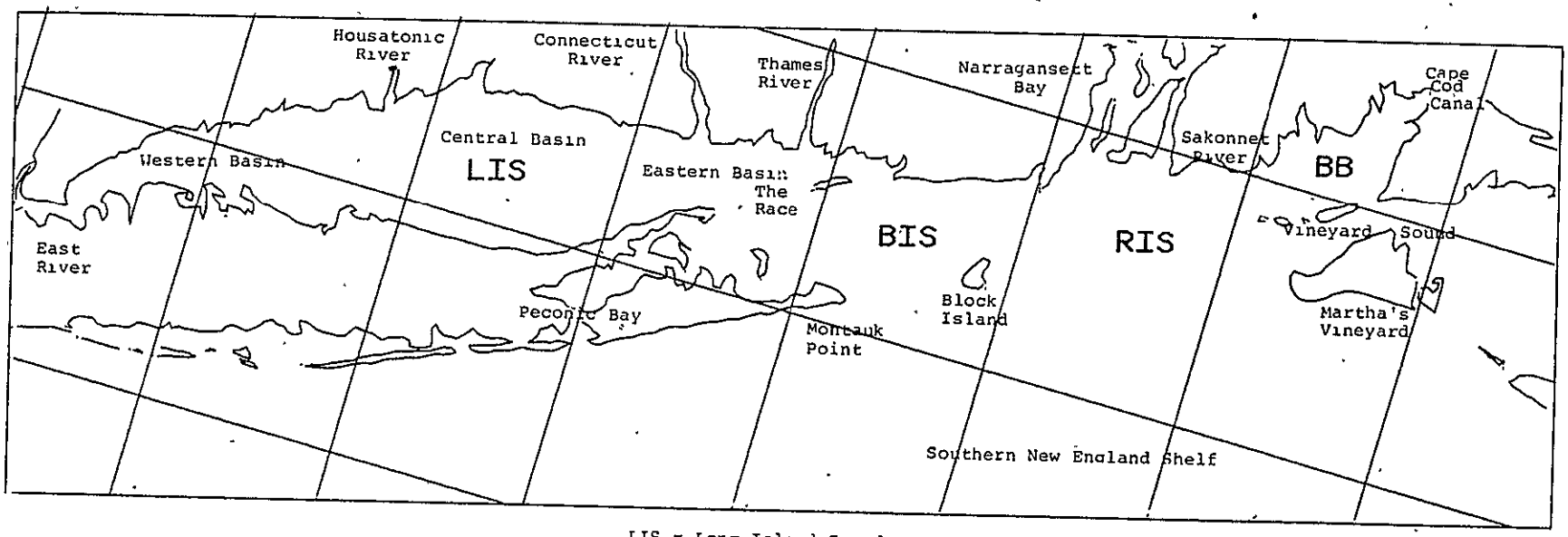

LIS = Long Island Sound
BIS = Block Island Sound
RIS = Rhode Island Sound
BB = Buzzards Bay

I.2 THE SOUTHERN NEW ENGLAND BIGHT.

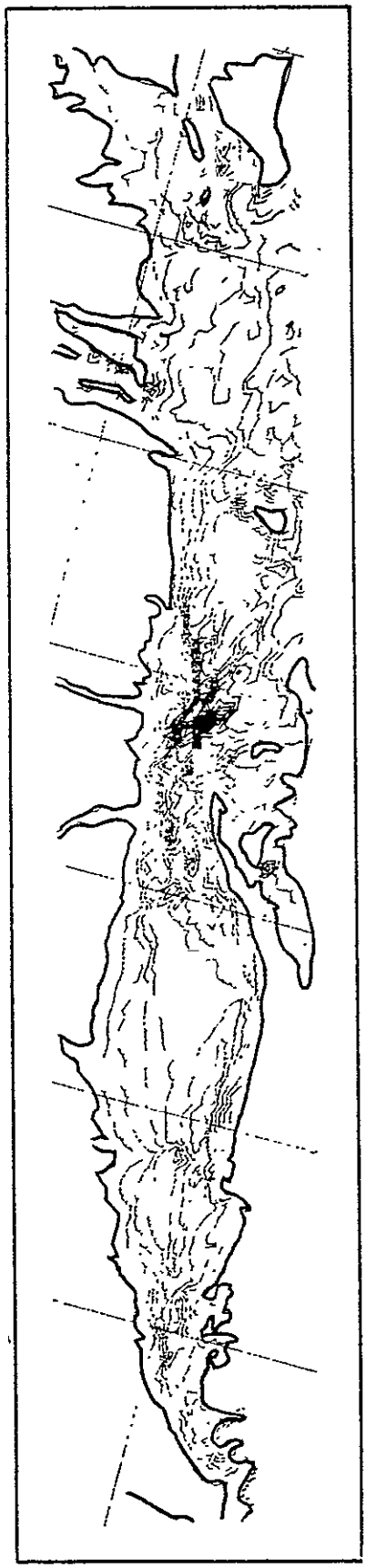

II.1 BOTTOM CONTOUR CHART OF THE SOUTHERN NEW ENGLAND BIGHT (MODEL BATHYMETRY).

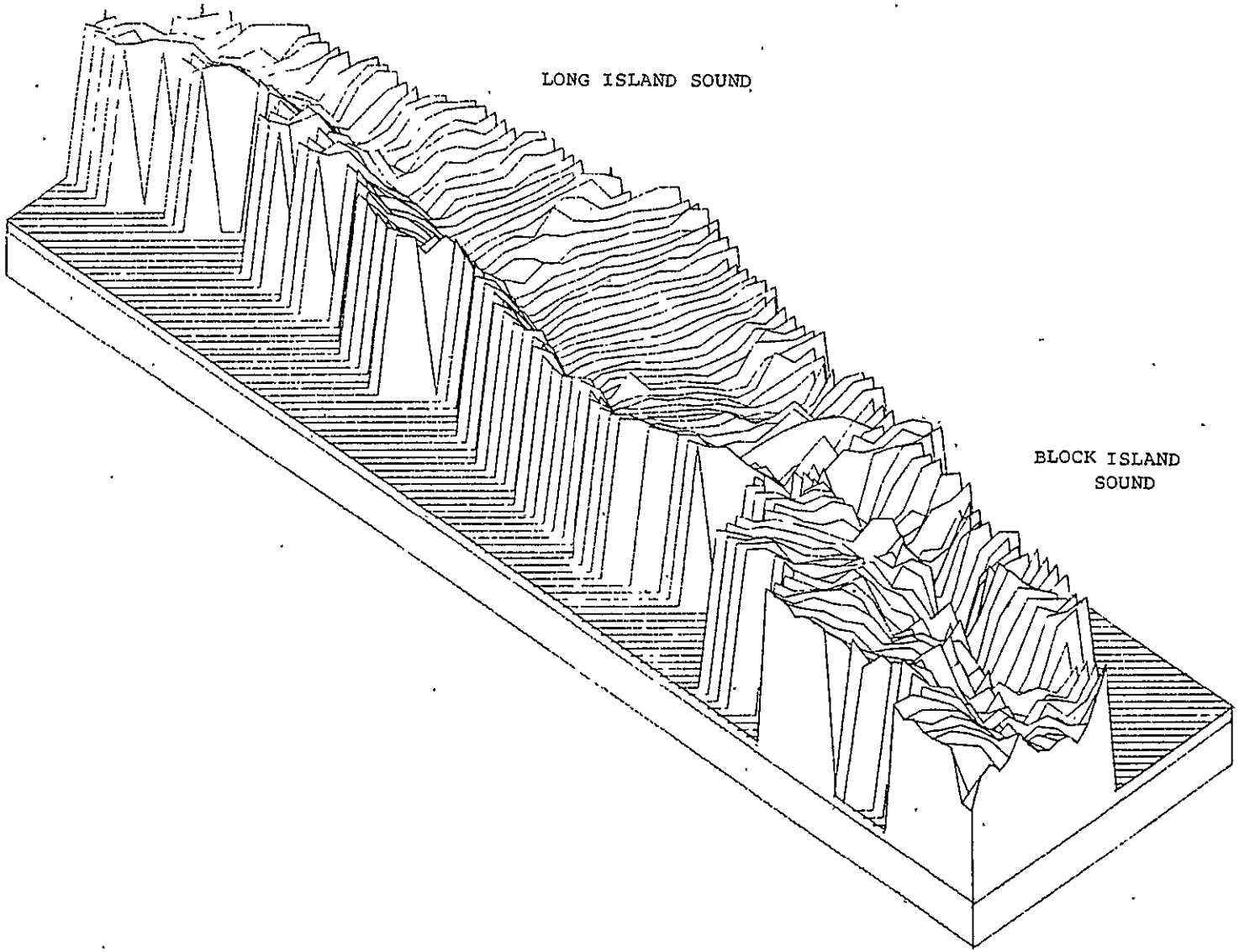

FIGURE II.2a THREE-DIMENSIONAL VIEW OF BATHYMETRY IN THE WESTERN PORTION OF THE SOUTHERN NEW ENGLAND BIGHT

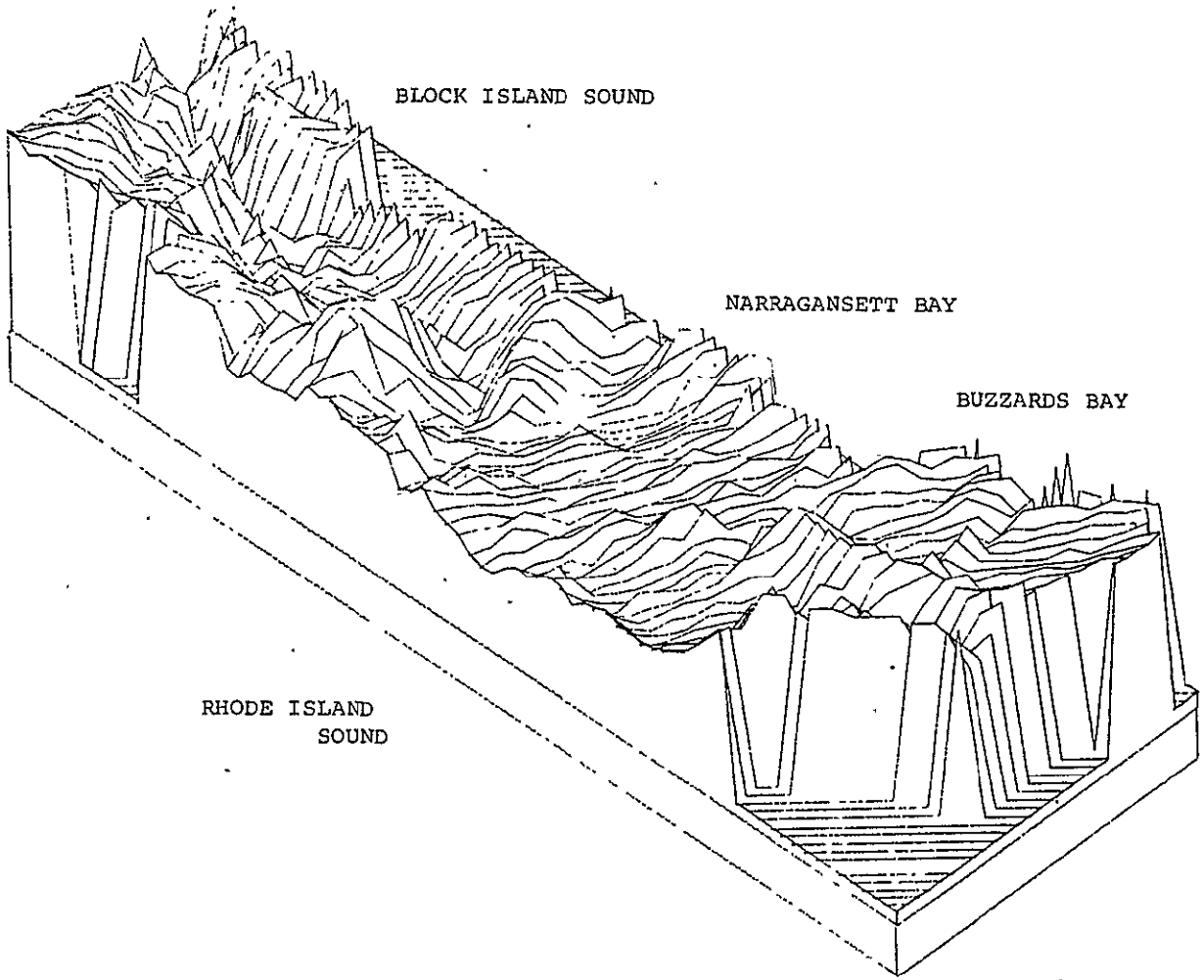

FIGURE II.2b THREE-DIMENSIONAL VIEW OF BATHYMETRY IN THE EASTERN PORTION OF THE SOUTHERN NEW ENGLAND BIGHT

TABLE II.1 SUMMARY OF OBSERVATIONS OF TIDES AND CURRENTS IN SOUTHERN NEW ENGLAND BIGHT

Reference	Variables* Measured	Location	Dates
Pruterch (1929)	V (Drifters)	Central Long Island Sound	--
Lelacheur & Sammons (1932)	ξ , V	Long Island and Block Island Sounds	Prior to 1932
Haight (1936)	ξ , V	Narragansett Bay, Buzzards Bay, Vineyard and Nantucket Sounds	Prior to 1936
Cook (1966)	V (Drifters)	Rhode Island Sound	--
Hicks (1967)	V	Long Island and Block Island Sounds	1965 - 1967
Larkin & Riley (1967)	V (Drifters)	Central Long Island Sound	--
Hicks (1968)	ξ	Rhode Island Sound, Buzzards Bay, Southern New England Shelf	August 1964
Shonting (1969)	V	Rhode Island Sound	1967
Hardy (1971)	V	Long Island Sound	--
Swanson (1971)	V	Eastern Long Island Sound	1965, 1976
Gross & Bumpus (1972)	V (Drifters)	Long Island Sound	March and October, 1969
Hollman & Sandberg (1972)	V (Drifters)	Eastern Long Island Sound, Block Island Sound	1970, 1971

* ξ surface elevation
V horizontal velocity

TABLE II.1 SUMMARY OF OBSERVATIONS OF TIDES AND CURRENTS IN SOUTHERN NEW ENGLAND BIGHT (CONT.)

Reference	Variables Measured	Location	Dates
Bohlen (1974)	V	Eastern Long Island Sound, Block Island Sound	--
Gordon & Pilbeam (1975)	V	Central Long Island Sound	1971, 1972, 1973
Raytheon (1975)	V	Block Island Sound	1975
Bowman (1976)	ξ , V	East River (Western Long Island Sound)	1959
Paskausky & Murphy (1976)	V (Drifters)	Long Island Sound	1973, 1974
Swanson (1976)	ξ	Long Island and Block Island Sounds, Southern New England Shelf	--
Beardsley, et al (1977)	ξ	Southern New England Shelf	Winter, 1974
Callaway (1977)	ξ	Southern New England Shelf	1973
Griscom (1977)	V	Rhode Island Sound	1976
Mofjeld (1977)	ξ	Southern New England Shelf	1975, 1976
NOS (1978)	ξ	Tide Tables	--
NOS (1978)	V	Tidal Current Tables	--

TABLE II.2 SUMMARY OF NUMERICAL CIRCULATION MODELS FOR SOUTHERN NEW ENGLAND BIGHT

Reference	Model Description-See Legend	Location of Application
Laevastu & Calla-way (1974)	H-2T-FD Explicit 6.6 km Grid Spacing	New York Bight Including Long Island & Block Island Sounds
Hurlbut & Spaulding (1975)	H-2T-FD Leendertse's Multi-Operational Scheme, 1.9 km Grid Spacing	Block Island Sound, Rhode Island Sound & Buzzards Bay
Lin & Skridulis (1975)	H-1T-FD & H-2T-FD Leendertse's Multi-Operational Scheme for Storm Surge	Long Island Sound
Wang & White (1976)	H-2T-FE & H-3T-FE, 3.7 km Node Spacing	Block Island Sound
Leendertse & Liu (1977)	H-3T-FD, 1.9 km Horizontal Grid Spacing	Long Island Sound
Beauchamp & Spaulding (1978)	H-2T-FD Leendertse's Multi-Operational Scheme, 1.9 km Grid Spacing	Southern New England Bight
Murphy (1978)	H-2T-FD Leendertse's Multi-Operational Scheme	Long Island Sound
Present Study	H-2T-FD Explicit (Greenberg's Method) Nested Grid, 5.6 km Grid Spacing on Shelf, 1.9 km Grid Spacing in Bight	Southern New England Bight & Part of New England Shelf

Legend:

H - Hydrodynamics
1T - One Dimensional, Transient
2T - Two Dimensional, Transient
3T - Three Dimensional, Transient
FD - Finite Difference
FE - Finite Element

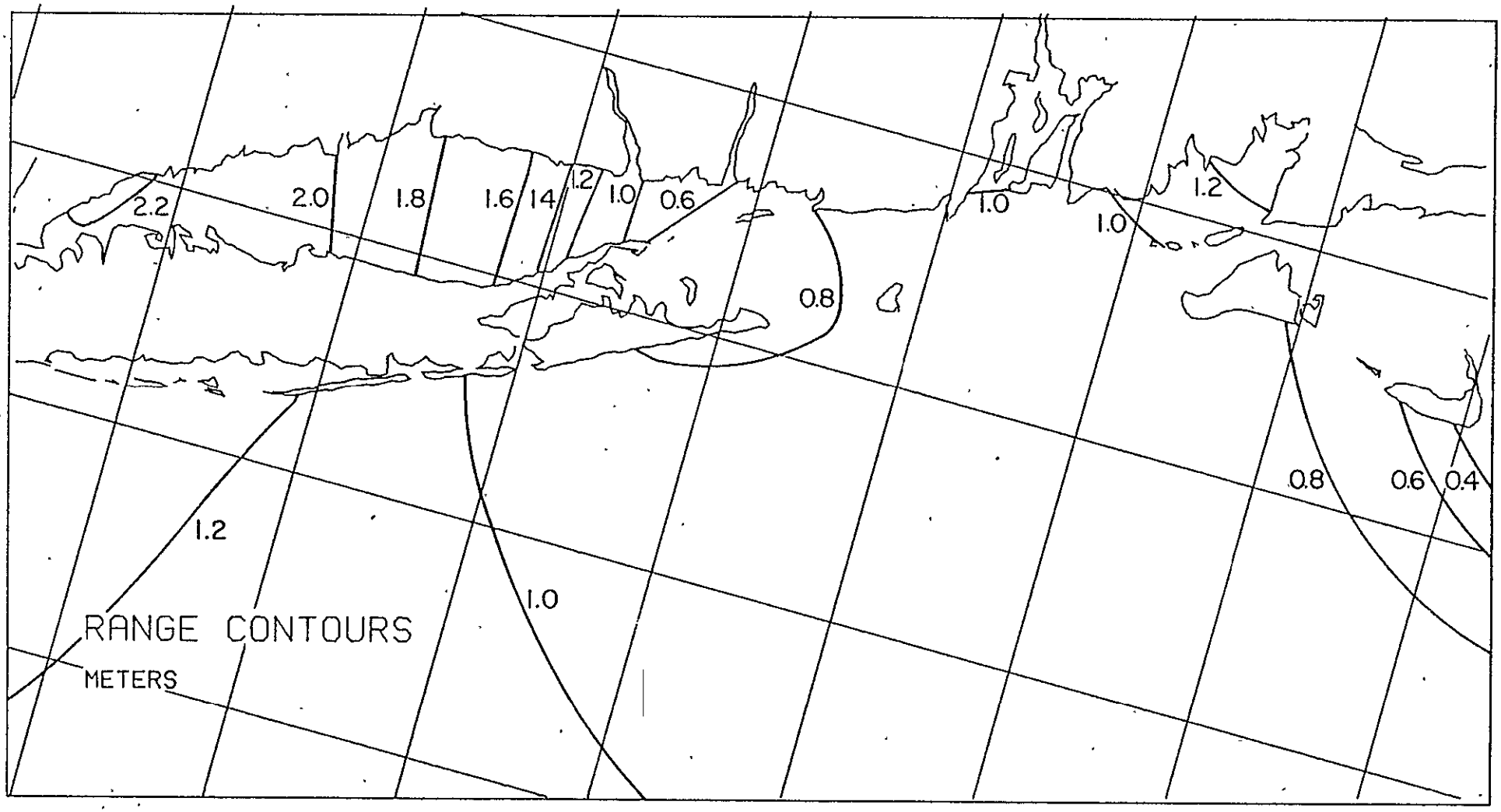

FIGURE II.3 OBSERVED CO-RANGE CHART OF THE STUDY AREA

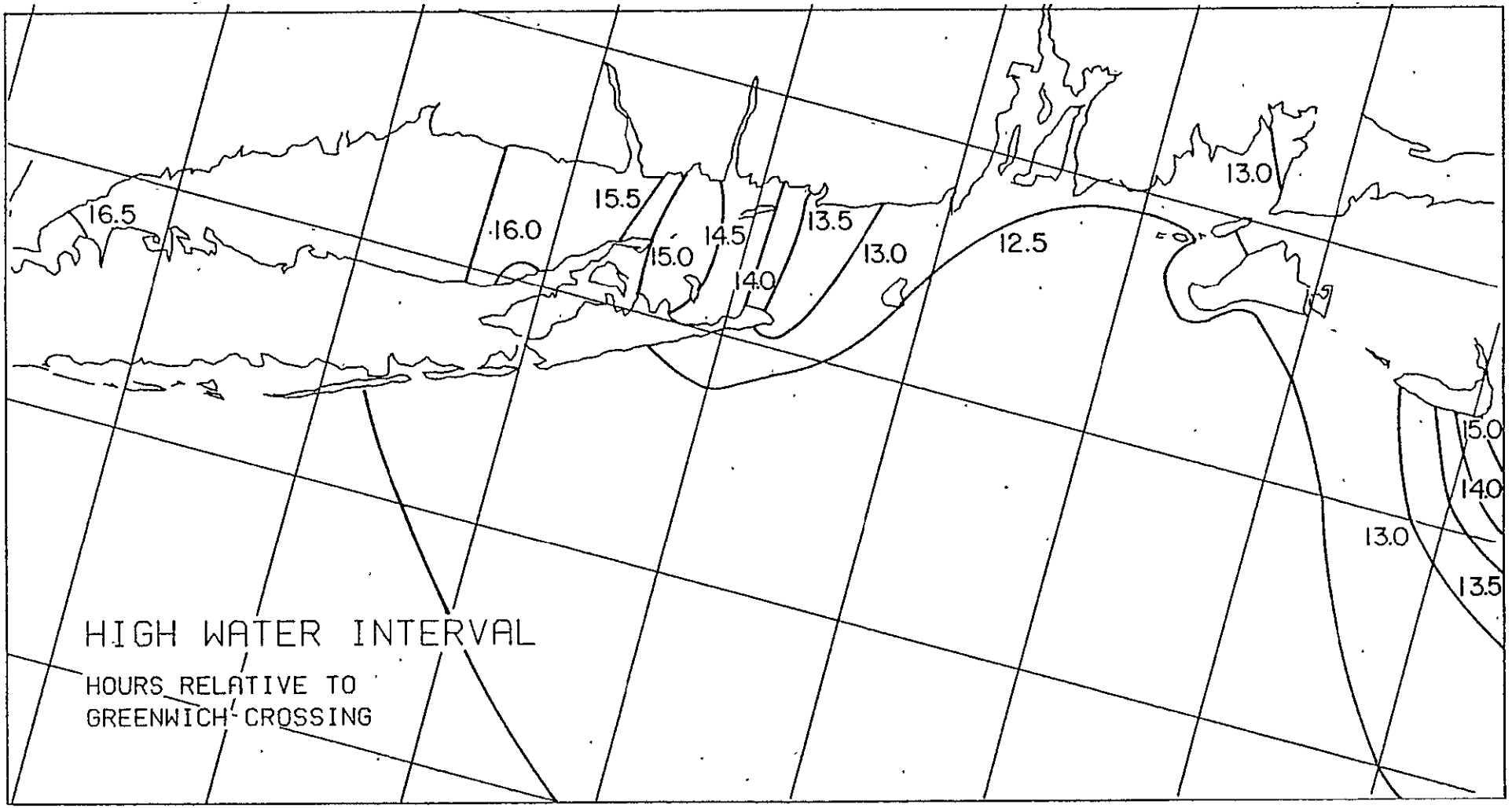

FIGURE II.4 OBSERVED GREENWICH HIGH WATER INTERVAL OF THE STUDY AREA

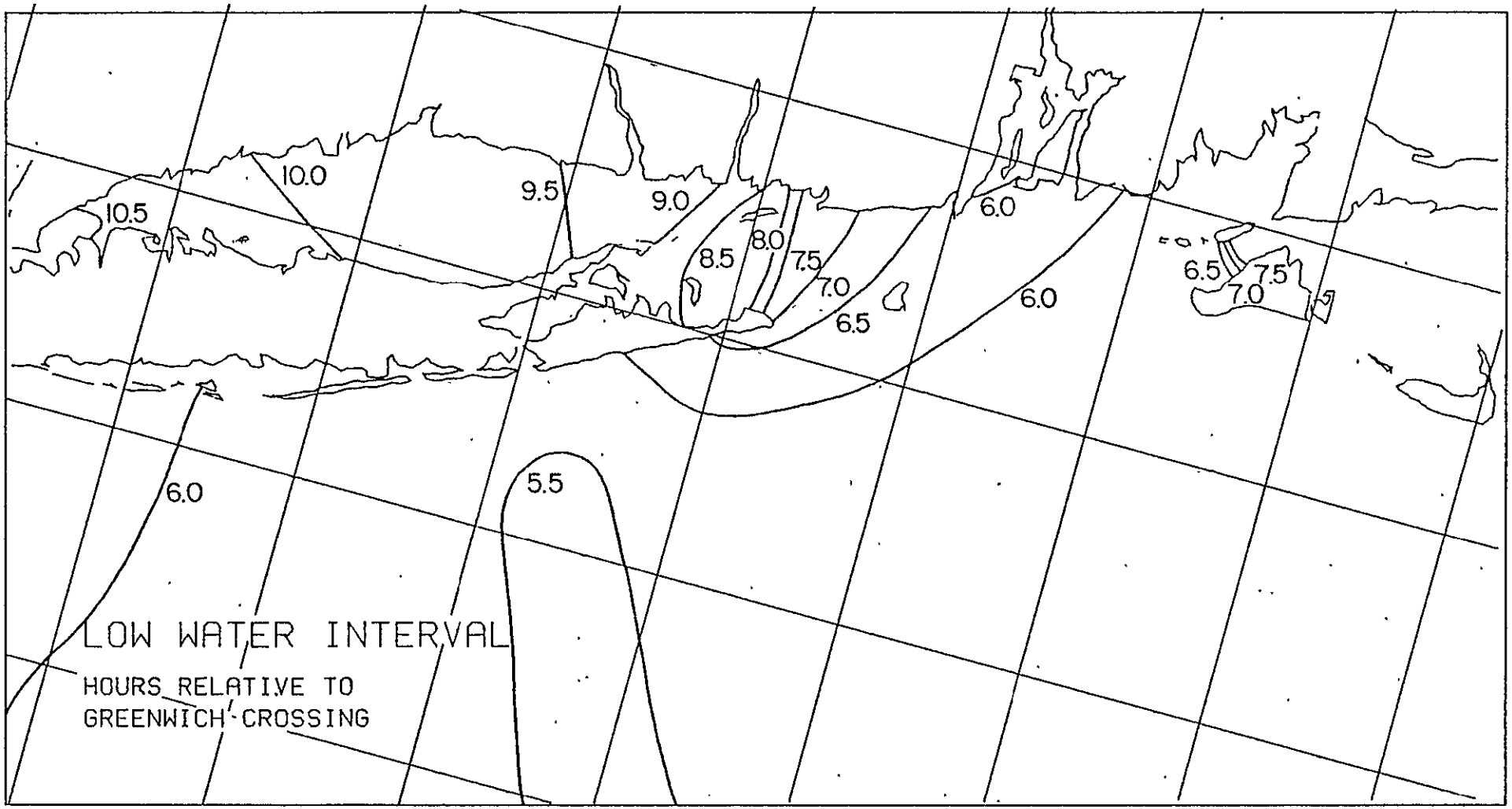

FIGURE II.5 OBSERVED GREENWICH LOW WATER INTERVAL OF THE STUDY AREA

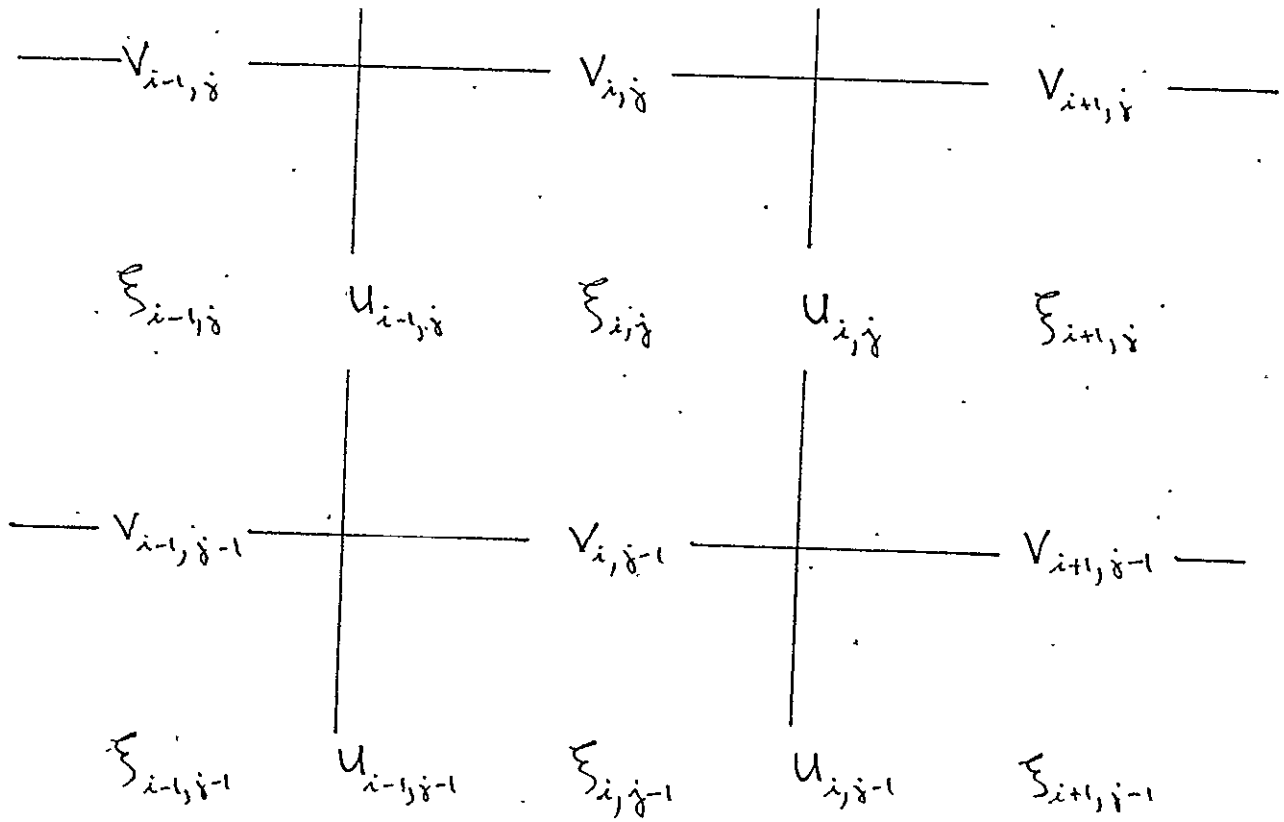

FIGURE III.1 FINITE DIFFERENCE GRID LAYOUT AND INDEXING

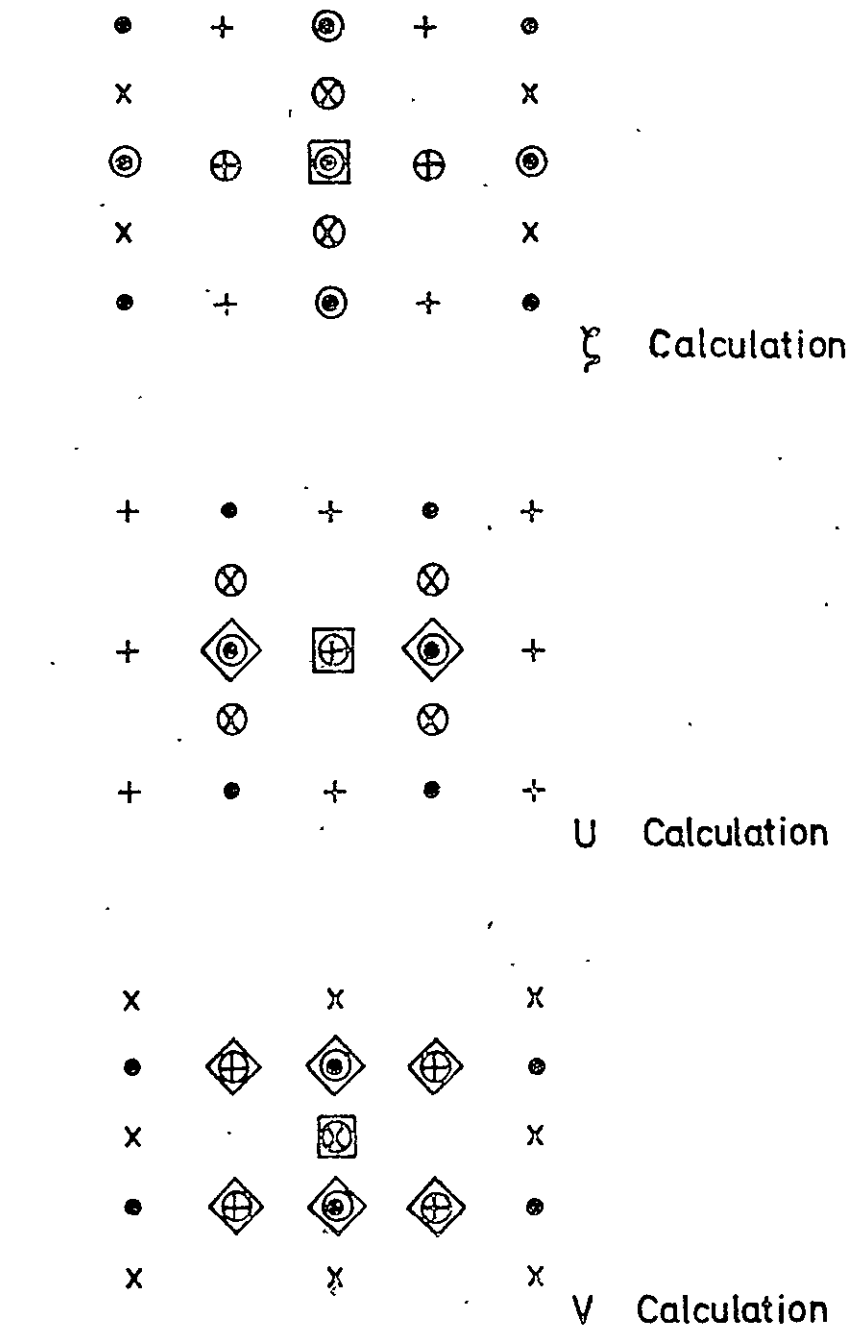

FIGURE III.2 CALCULATION PROCEDURE FOR SURFACE ELEVATION AND HORIZONTAL VELOCITY COMPONENTS (FROM GREENBERG (1977))

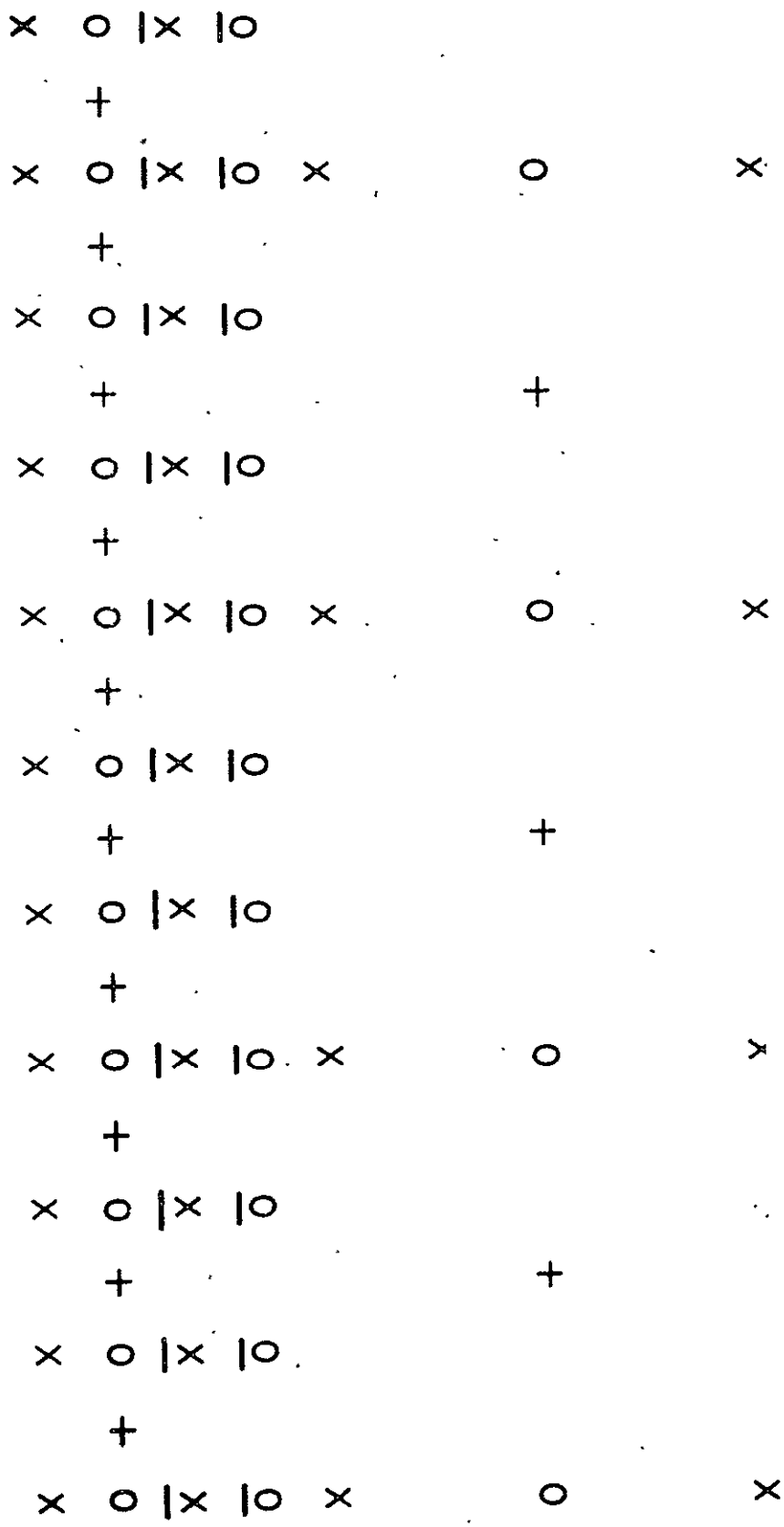

FIGURE III.3 COARSE-FINE GRID INTERFACE (SEE FIG. III.2 FOR EXPLANATION OF SYMBOLS). POINTS UNDERLINED ARE THOSE OBTAINED BY INTERPOLATION (FROM GREENBERG (1977))

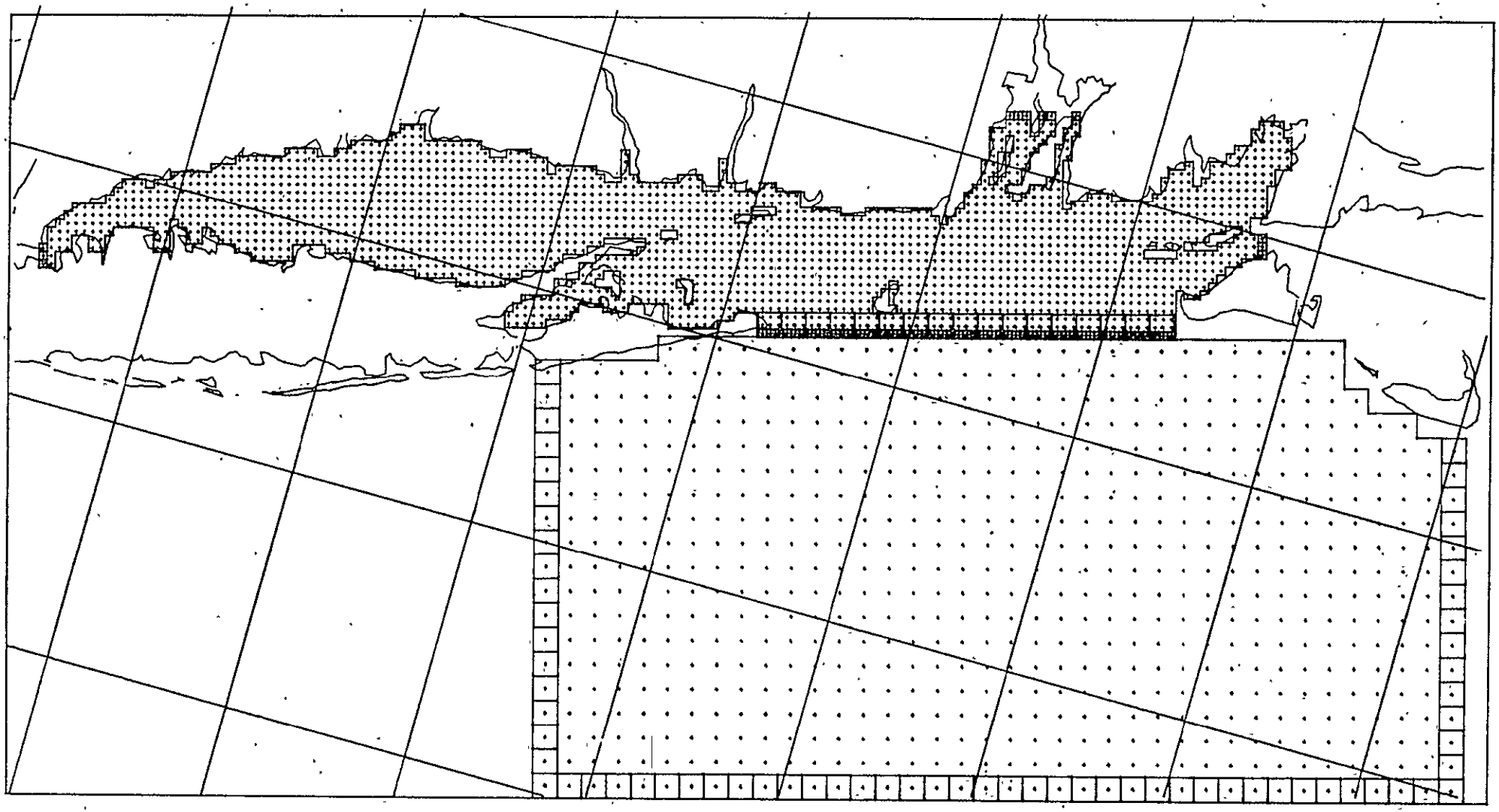

FIGURE III.4 THE NESTED FINITE DIFFERENCE GRID SYSTEM. SPACING FOR THE THREE GRIDS ARE 3, 1 AND 1/3 NAUTICAL MILES

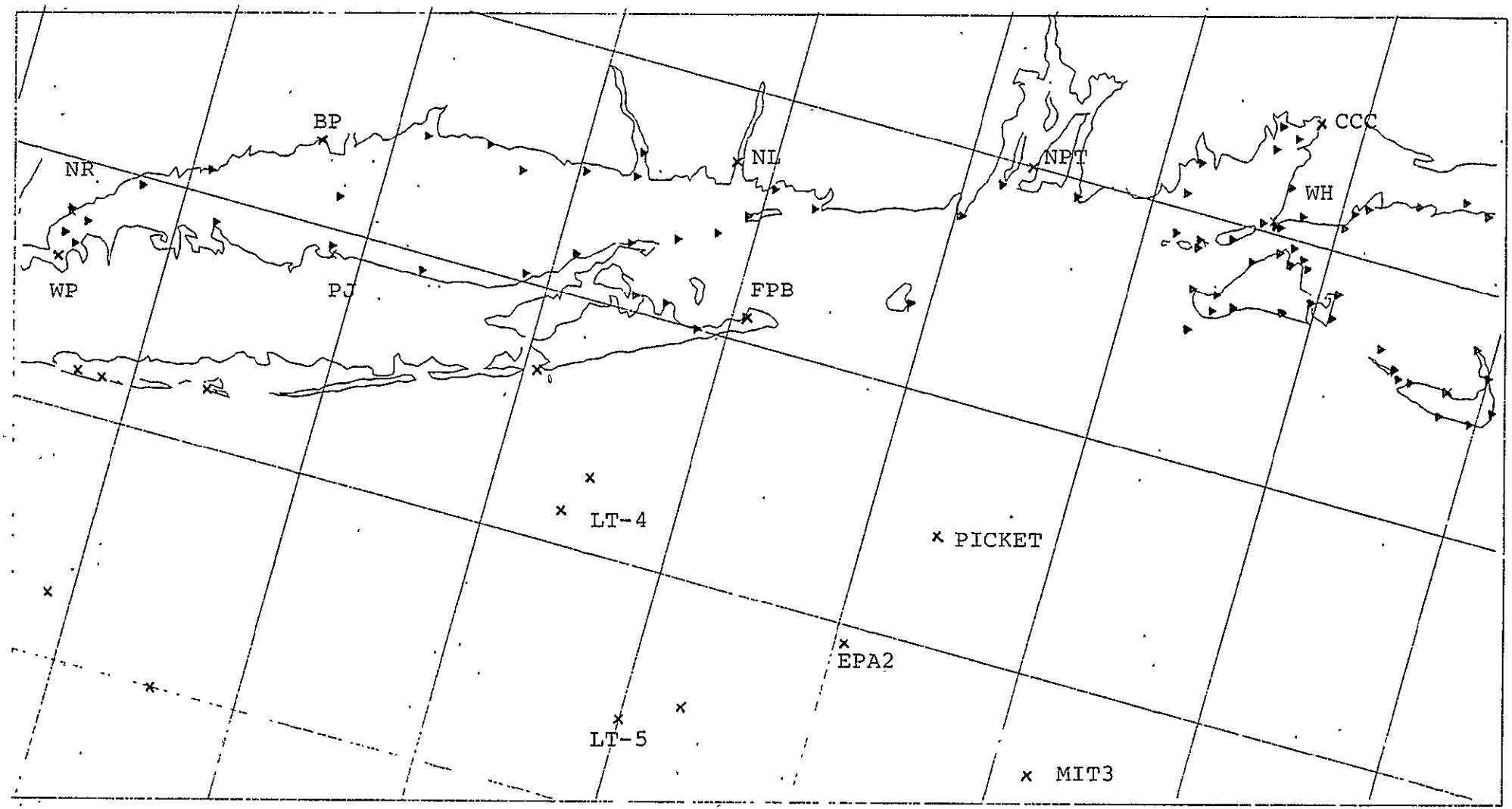

III.5 LOCATION OF TIDE STATIONS.

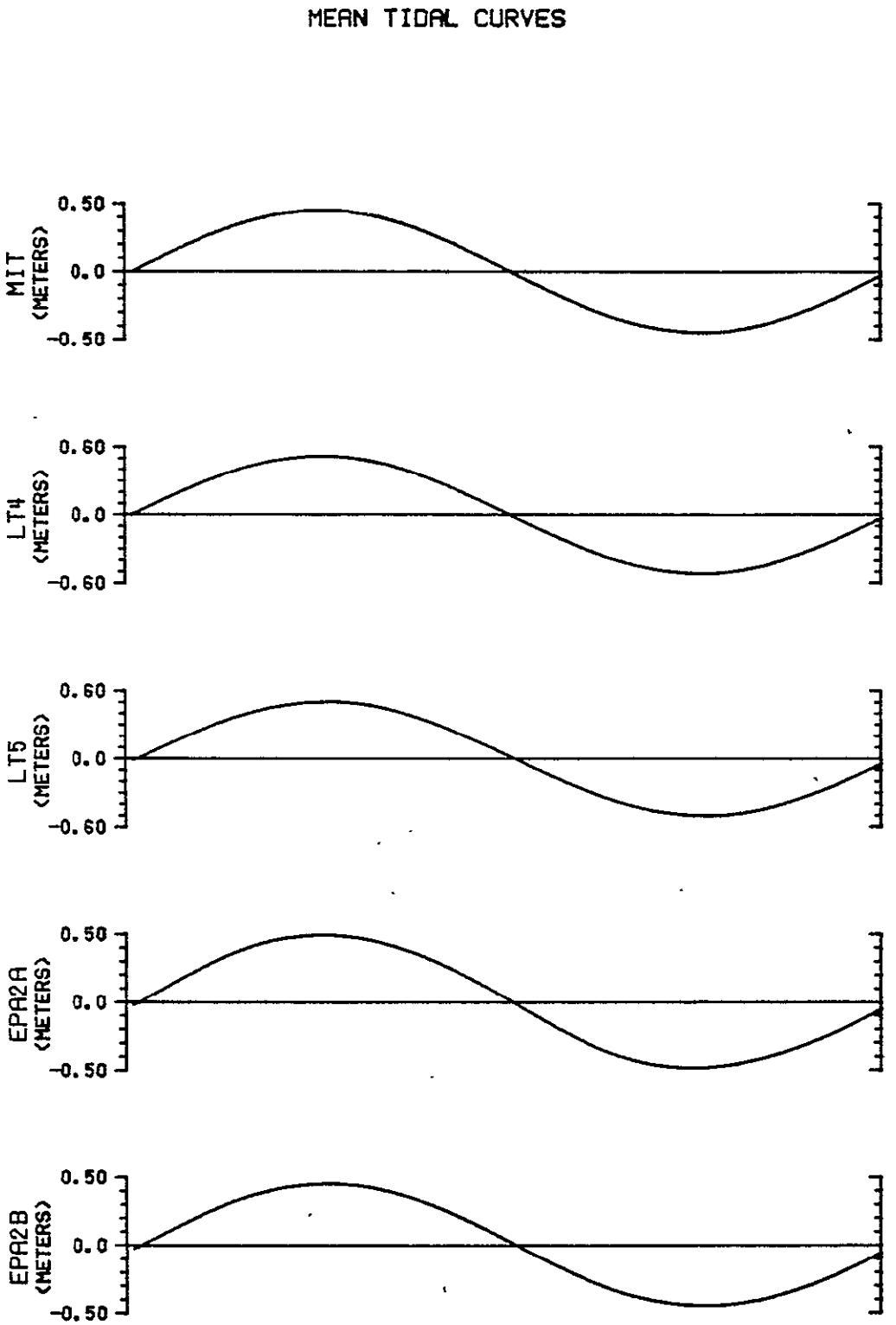

III.6 MEAN TIDE CURVES USED AS INPUT BOUNDARY CONDITIONS.

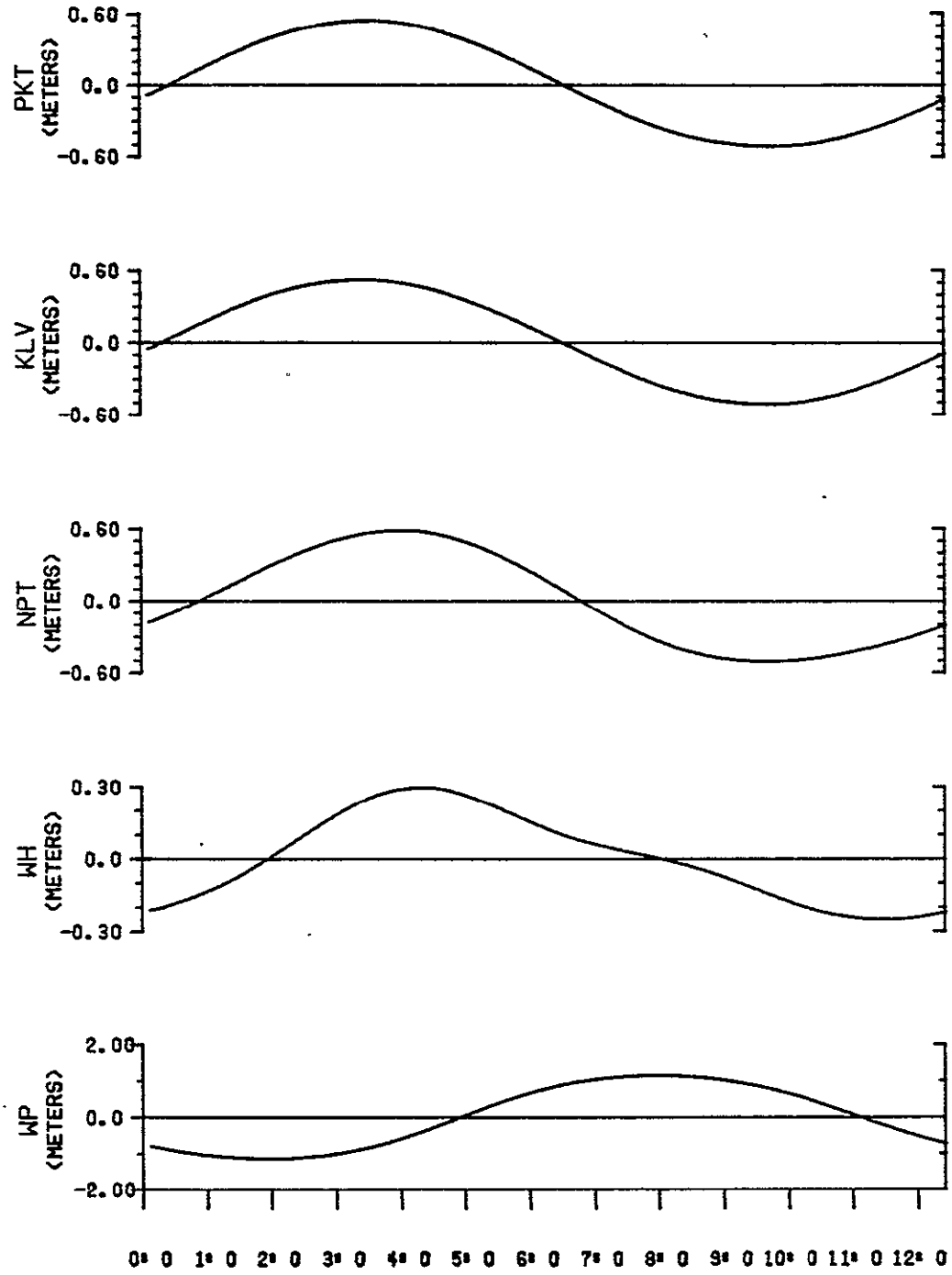

III.6 MEAN TIDE CURVES USED AS INPUT BOUNDARY CONDITIONS. (CONT.)

TABLE III.1

AMPLITUDE AND PHASE OF THE MAJOR TIDAL CONSTITUENTS FOR LOCATIONS USED AS MODEL BOUNDARY CONDITIONS

	DIURNAL				SEMI-DIURNAL				QUARTER-DIURNAL		SIXTH-DIURNAL		
	K_1		O_1		N_2		M_2		M_4		M_6		
Station	H(m.)	K(°)	H	K	H	K	H	K	H	K	H	K	R
Woods Hole	0.065	114.1	0.065	133.6	0.077	239.2	0.236	250.6	0.049	65.5	0.019	333.9	0.44
Willets Point	0.101	119.0	0.061	130.0	0.231	306.0	1.119	329.0	0.032	214.0	0.071	83.0	0.12
MIT3	0.083	97.8	0.068	108.3	0.105	184.8	0.422	202.1	--	--	--	--	0.29
EPA2A	0.080	84.4	0.052	113.0	0.091	191.2	0.467	202.6	0.010	92.9	0.010	137.5	0.25
EPA2B	0.066	83.5	0.037	92.5	0.083	191.0	0.431	204.6	0.003	54.5	0.004	117.5	0.24
LT4	0.080	90.4	0.056	110.5	0.120	187.9	0.485	201.6	--	--	--	--	0.23
LT5	0.084	99.9	0.060	114.7	0.113	189.0	0.471	203.9	--	--	--	--	0.27
Picket	0.077	79.2	0.061	120.1	0.121	192.3	0.495	209.6	0.014	61.1	0.006	112.0	0.23
Kelvin	0.093	91.5	0.080	112.8	0.115	189.1	0.465	207.6	0.004	12.5	0.002	133.5	0.30

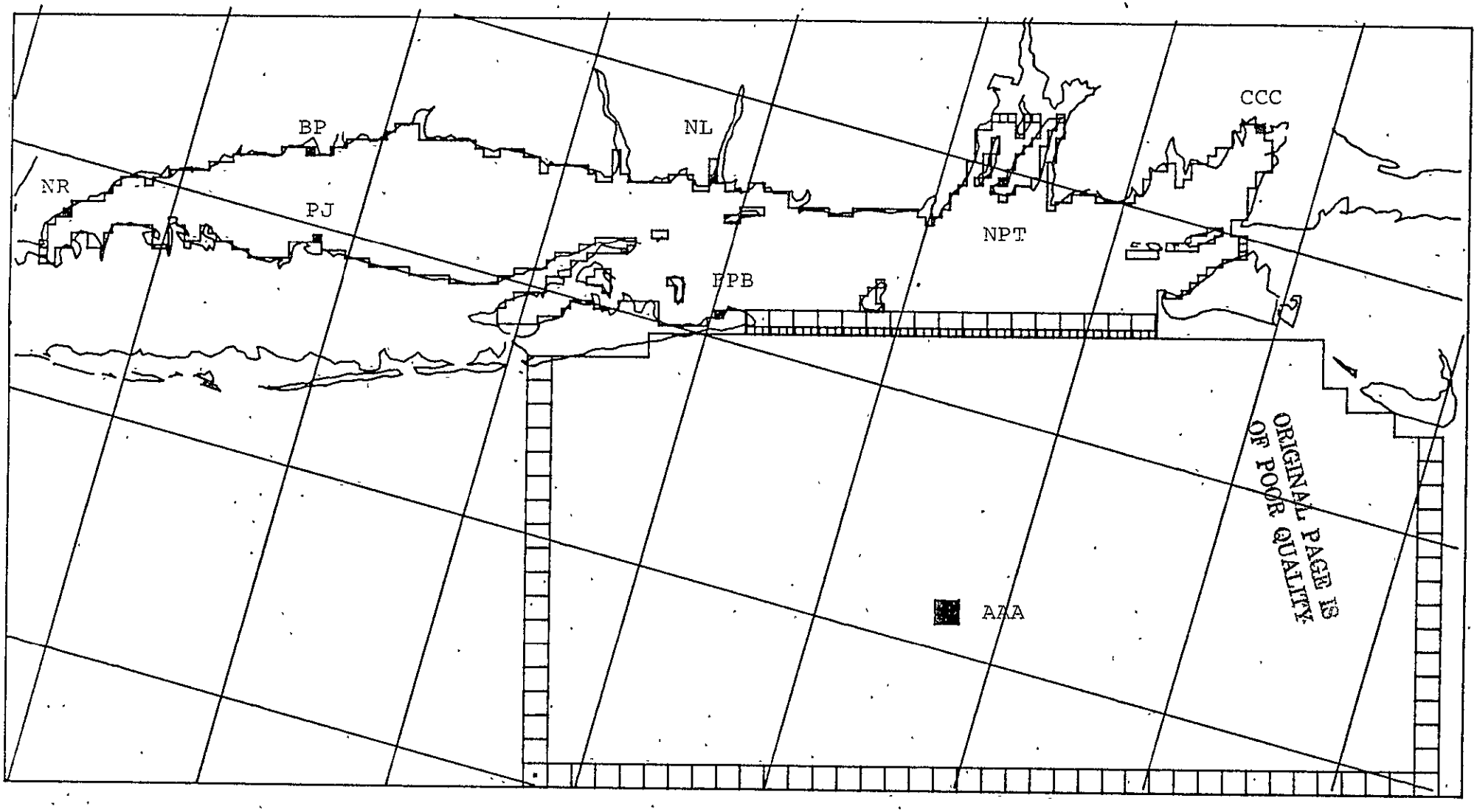

FIGURE IV.1 LOCATION OF STATIONS WITHIN THE MODEL GRID FOR WHICH SURFACE ELEVATION TIME HISTORIES ARE PLOTTED

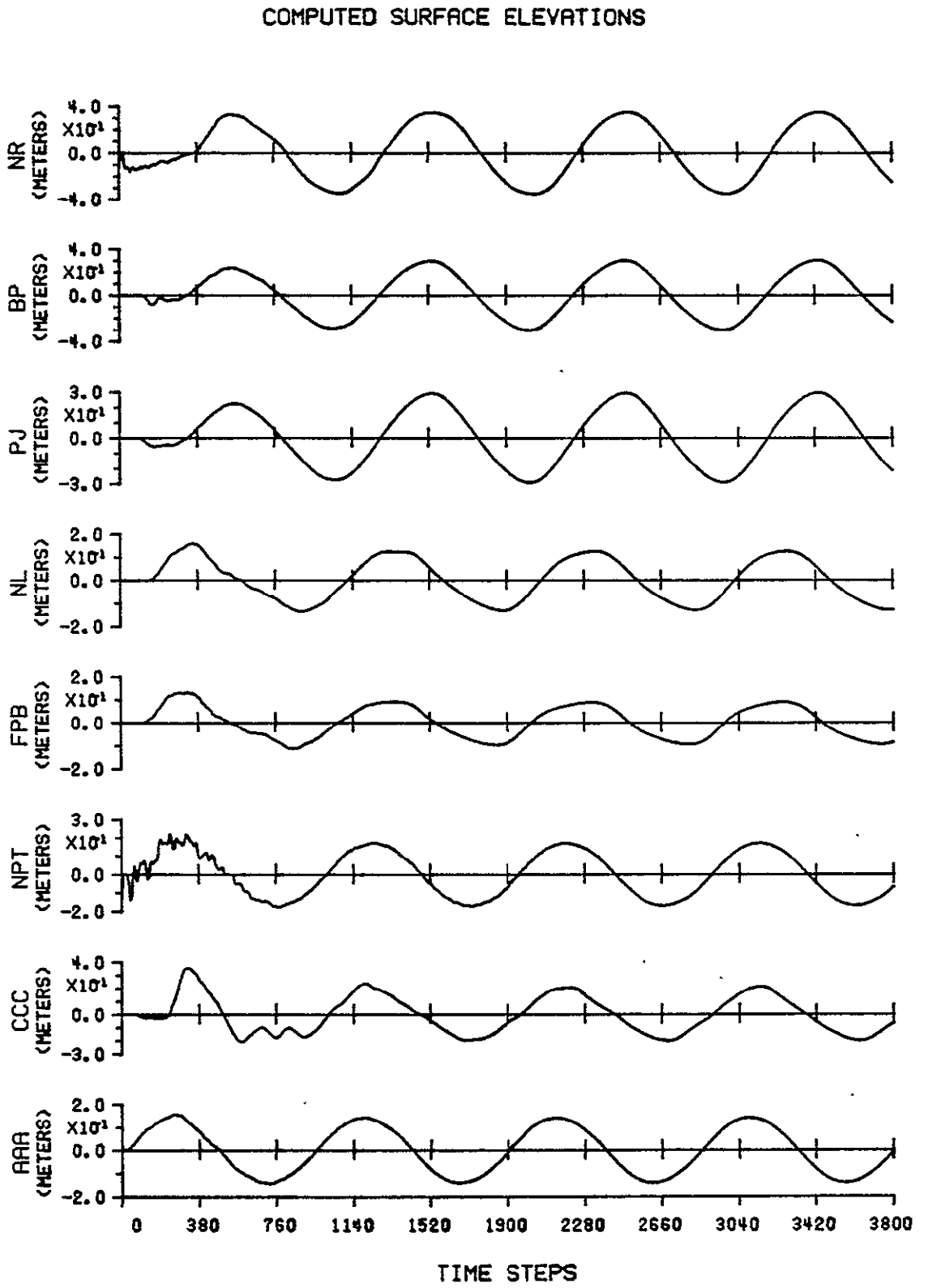

IV.2 COMPUTED SURFACE ELEVATION TIME HISTORIES FOR VARIOUS LOCATIONS IN THE STUDY AREA.

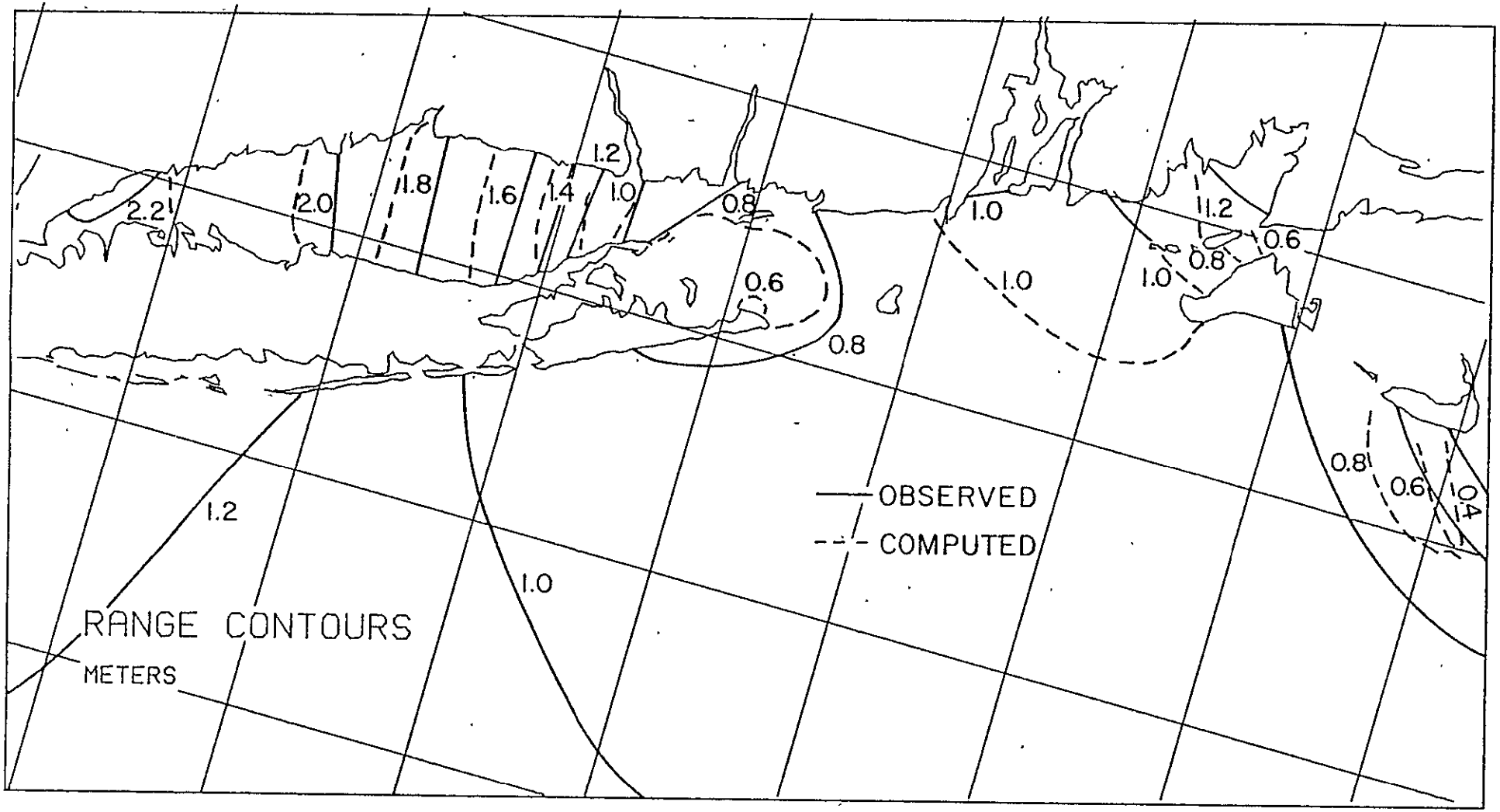

FIGURE IV.3 COMPUTED AND OBSERVED CO-RANGE CHART OF THE STUDY AREA

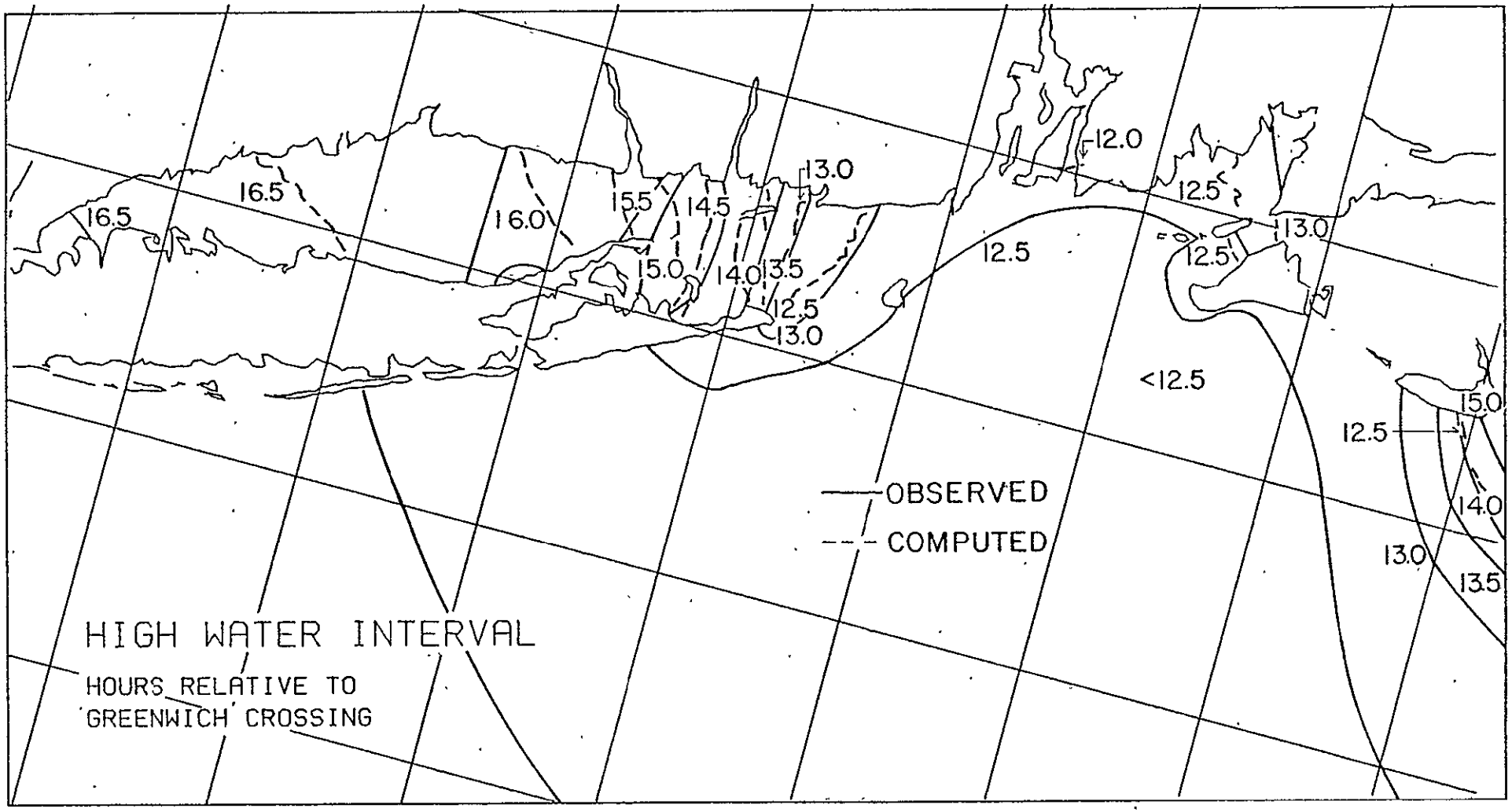

FIGURE IV.4 COMPUTED AND OBSERVED GREENWICH HIGH WATER INTERVAL CHART OF THE STUDY AREA

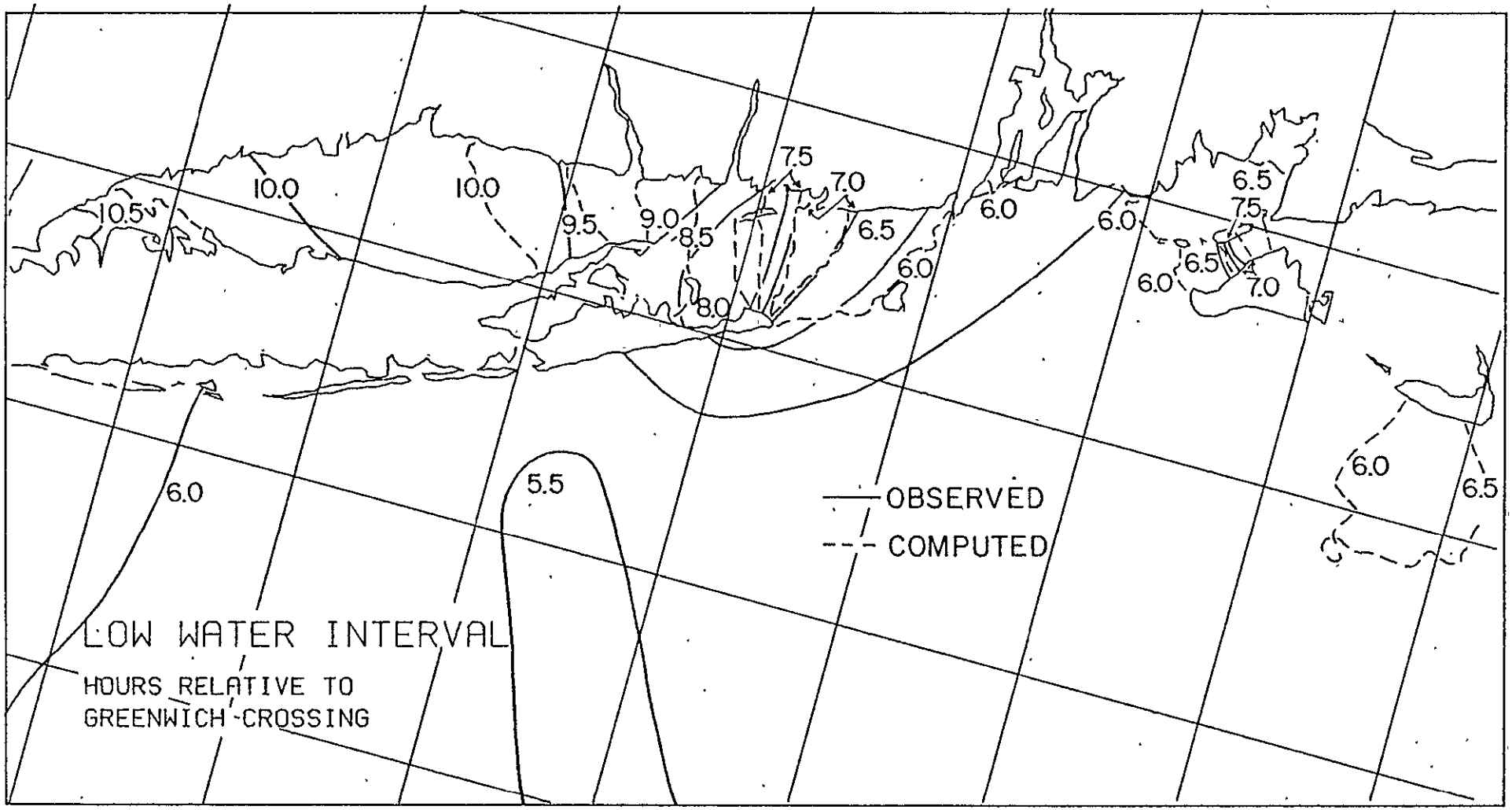

FIGURE IV.5 COMPUTED AND OBSERVED GREENWICH LOW WATER INTERVAL CHART OF THE STUDY AREA

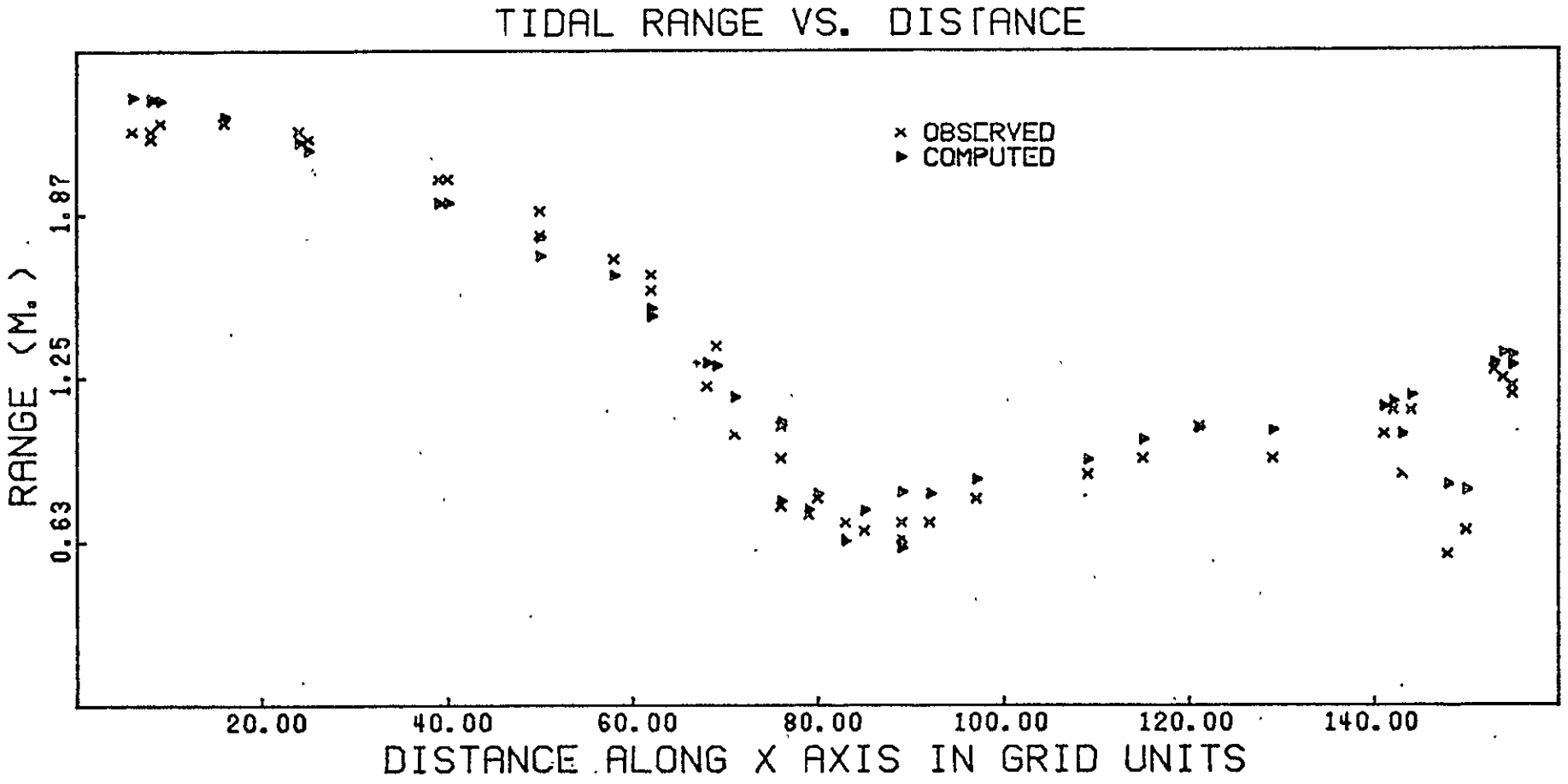

IV.6 OBSERVED AND COMPUTED TIDAL RANGE VS. MODEL X-AXIS DISTANCE. (1 GRID UNIT = 1.9 KM).

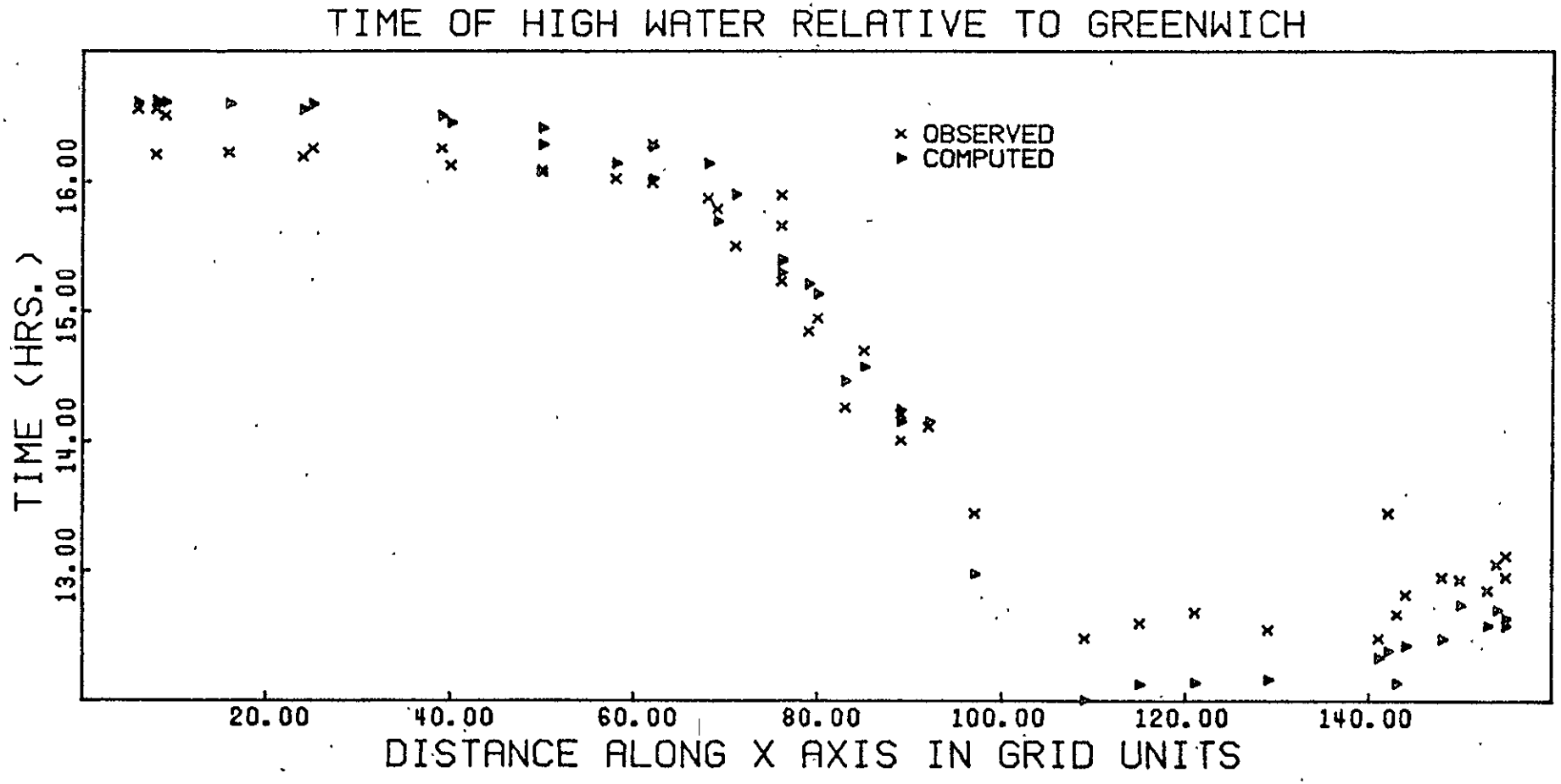

IV.7 OBSERVED AND COMPUTED HIGH WATER INTERVAL VS. MODEL X-AXIS DISTANCE. (1 GRID UNIT = 1.9 KM)

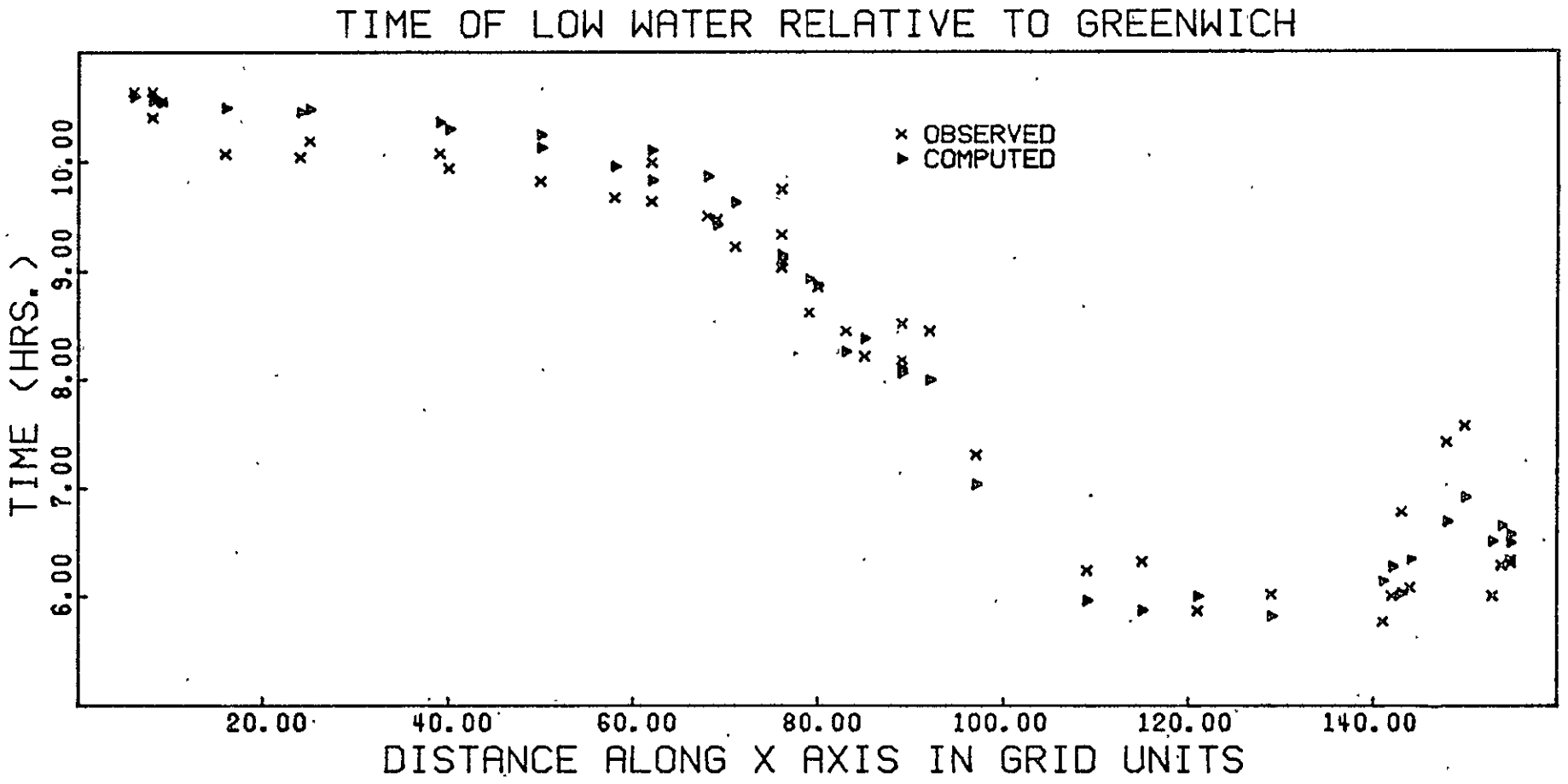

IV.8 OBSERVED AND COMPUTED LOW WATER INTERVAL VS. MODEL X-AXIS DISTANCE. (1 GRID UNIT = 1.9 KM).

TABLE IV.1

COMPARISON OF OBSERVED (NOS TIDE STATIONS) AND COMPUTED TIDAL RANGE AND PHASE

	I	J	ID #	STATION	LAT	LONG	RANGE (M)			HIGH WATER INTERVAL (HR.)			LOW WATER INTERVAL (HR.)		
							OBS	COMP	DIFF	OBS	COMP	DIFF	OBS	COMP	DIFF
1	183	6	1069	GAY HEAD	41 21	70 50	0.88	1.04	0.15	12.67	12.14	0.53	6.79	6.04	0.76
2	150	10	1073	CEDAR TREE NECK	41 26	70 47	0.67	0.82	0.15	12.94	12.74	0.19	7.58	6.93	0.65
3	148	11	1097	TARPAULIN COVE	41 28	70 46	0.58	0.84	0.27	12.95	12.48	0.47	7.43	6.70	0.72
4	141	13	1107	PENIKESE ISLAND	41 27	70 55	1.04	1.14	0.10	12.49	12.34	0.15	5.78	6.15	0.38
5	155	20	1111	WEST FALMOUTH HARBOR	41 36	70 39	1.22	1.30	0.08	13.12	12.59	0.53	6.34	6.51	0.16
6	155	25	1115	ABIPLS LEDGE	41 42	70 40	1.19	1.34	0.15	12.95	12.64	0.31	6.31	6.59	0.28
7	154	26	1121	GREAT HILL	41 43	70 43	1.25	1.34	0.09	13.05	12.70	0.35	6.29	6.66	0.37
8	153	23	1125	BIRD ISLAND	41 40	70 43	1.28	1.31	0.03	12.85	12.59	0.27	6.01	6.52	0.51
9	144	21	1133	CLARKS POINT	41 36	70 54	1.13	1.19	0.06	12.82	12.43	0.39	6.09	6.35	0.26
10	142	18	1141	DUMPING ROCKS	41 32	70 55	1.13	1.16	0.04	13.45	12.39	1.06	6.01	6.29	0.28
11	129	17	1147	SAKONNET	41 28	71 12	0.94	1.05	0.11	12.55	12.17	0.38	6.03	5.83	0.20
12	121	19	1151	BEAVERTAIL POINT	41 27	71 24	1.07	1.06	0.00	12.69	12.14	0.54	5.88	6.01	0.13
13	115	18	1179	POINT JUDITH HARBOR	41 22	71 29	0.94	1.02	0.07	12.60	12.13	0.47	6.33	5.88	0.45
14	109	5	1183	BLOCK ISALND (OLD HA	41 10	71 31	0.88	0.94	0.06	12.49	12.01	0.47	6.24	5.97	0.27
15	97	16	1185	WATCH HILL POINT	41 18	71 52	0.79	0.87	0.07	13.45	12.98	0.47	7.31	7.04	0.27
16	92	18	1189	NOANK, MYSTIC RIVER	41 19	71 59	0.70	0.81	0.11	14.12	14.16	0.04	8.45	8.00	0.45
17	89	15	1192	SILVER EEL POND, FIS	41 15	72 2	0.70	0.82	0.12	14.22	14.16	0.06	8.51	8.06	0.45
18	76	20	1200	SAYBROOK JETTY	41 16	72 21	1.07	1.07	0.01	15.67	15.40	0.27	9.33	9.15	0.18
19	76	22	1202	LYME, HIGHWAY BRIDGE	41 19	72 21	0.94	1.08	0.14	15.90	15.41	0.49	9.75	9.11	0.64
20	69	20	1215	DUCK ISLAND	41 15	72 29	1.37	1.30	0.07	15.79	15.70	0.09	9.47	9.42	0.05
21	62	20	1219	FAIRHEP ISLAND	41 13	72 39	1.65	1.52	0.13	15.99	16.03	0.03	9.64	9.83	0.19
22	58	23	1221	MONEY ISLAND	41 15	72 45	1.71	1.64	0.06	16.03	16.14	0.12	9.67	9.96	0.29
23	50	24	1225	NEW HAVEN HARBOR ENT	41 18	72 55	1.89	1.79	0.10	16.08	16.29	0.21	9.82	10.13	0.31
24	29	20	1243	GREENS LEDGE	41 3	73 27	2.19	2.15	0.04	16.19	16.56	0.37	10.08	10.46	0.42
25	15	18	1251	GREAT CAPTAIN ISLAND	40 59	73 37	2.23	2.25	0.02	16.23	16.60	0.37	10.07	10.50	0.42
26	8	15	1257	PEW ROCKPILE	40 58	73 47	2.19	2.32	0.12	16.21	16.61	0.40	10.41	10.56	0.15
27	6	12	1261	CITY ISLAND	40 51	73 47	2.19	2.33	0.13	16.56	16.61	0.05	10.64	10.60	0.04
28	9	11	1333	HEWLETT POINT	40 50	73 45	2.16	2.31	0.15	16.56	16.63	0.07	10.64	10.60	0.04

TABLE IV.1 (CONT.)

COMPARISON OF OBSERVED (NOS TIDE STATIONS) AND COMPUTED TIDAL RANGE AND PHASE

29	9	14	1337	EXPCOTTON ROCKS	40	53	73	44	2.23	2.31	0.09	16.51	16.61	0.10	10.56	10.55	0.01
30	25	14	1347	EATONS NECK POINT	40	57	73	24	2.16	2.12	0.04	16.26	16.60	0.34	10.19	10.48	0.29
31	40	17	1357	STRATFORD SHOAL	41	4	73	6	2.01	1.92	0.09	16.13	16.46	0.33	9.98	10.30	0.36
32	39	12	1359	PORT JEFFERSON HARBO	40	58	73	5	2.01	1.92	0.09	16.26	16.51	0.25	10.07	10.36	0.29
33	50	9	1369	HEROD DAY	40	58	72	50	1.80	1.72	0.08	16.09	16.42	0.32	9.82	10.25	0.42
34	62	8	1371	MATTITUCK INLET	41	1	72	34	1.58	1.49	0.10	16.29	16.27	0.02	9.99	10.10	0.11
35	68	10	1373	HORTON POINT	41	5	72	27	1.22	1.31	0.09	15.88	16.14	0.27	9.51	9.87	0.36
36	71	11	1375	TRUMAN BEACH	41	8	72	19	1.04	1.18	0.14	15.51	15.91	0.40	9.22	9.63	0.41
37	80	12	1377	PLUM GUT HARBOR, PLU	41	10	72	12	0.79	0.81	0.02	14.95	15.14	0.19	8.85	8.86	0.01
38	85	13	1379	LITTLE GULL ISLAND	41	12	72	6	0.67	0.75	0.08	14.70	14.57	0.13	8.21	8.38	0.16
39	76	5	1391	CEDAR POINT	41	2	72	16	0.76	0.78	0.02	15.23	15.31	0.07	9.03	9.06	0.03
40	79	5	1399	THREEMILE HBR., GARD	41	2	72	11	0.73	0.75	0.02	14.85	15.21	0.36	8.61	8.93	0.31
41	83	2	1401	PROMISED LAND, NAPEA	41	0	72	5	0.70	0.63	0.07	14.27	14.47	0.20	8.45	8.26	0.19
42	89	3	1405	MONTAUK, FORT POND B	41	3	71	58	0.64	0.61	0.03	14.02	14.25	0.23	8.18	8.10	0.08

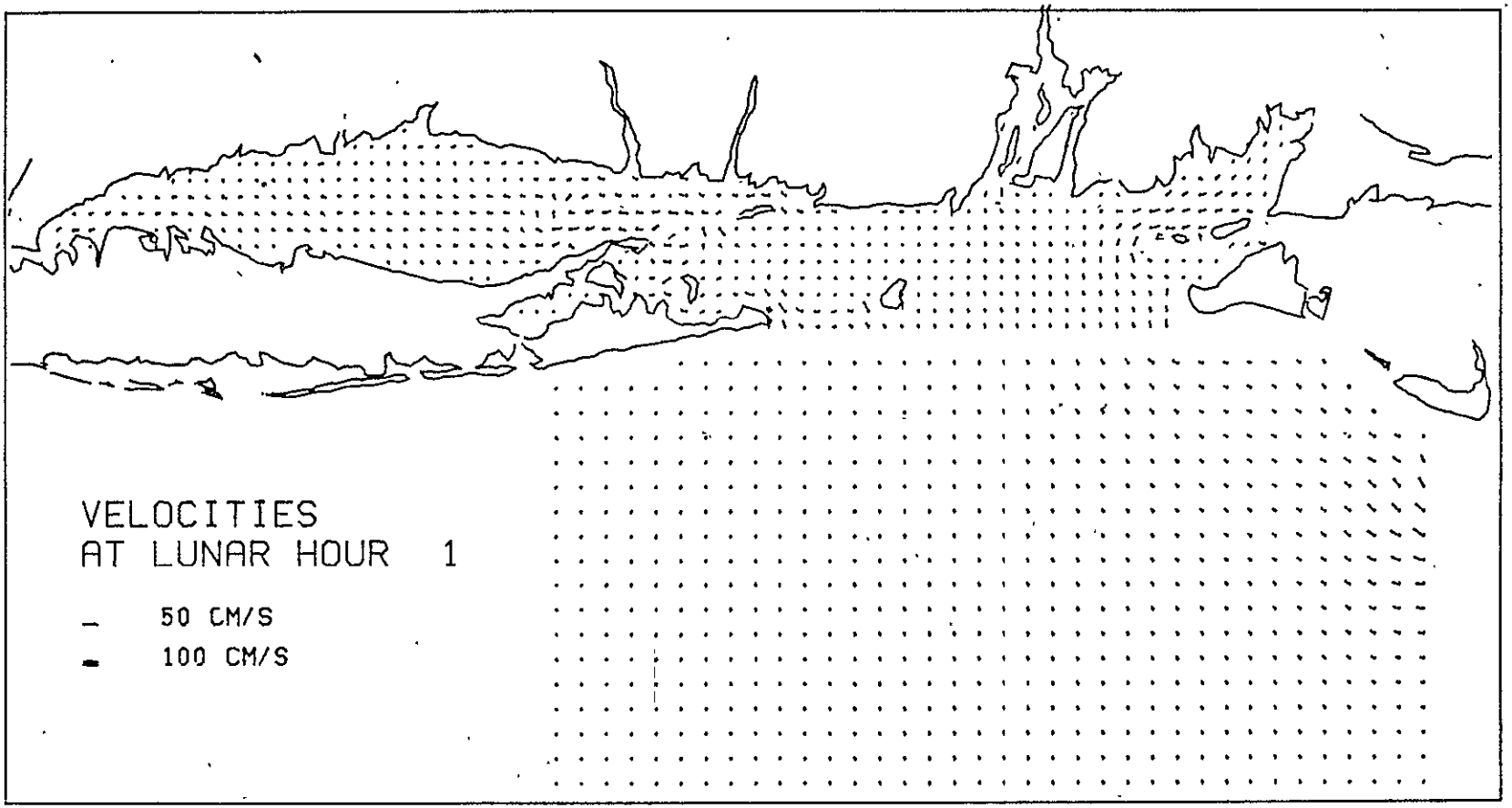

IV.9 COMPUTED VELOCITY VECTORS AT LUNAR HOUR 1.

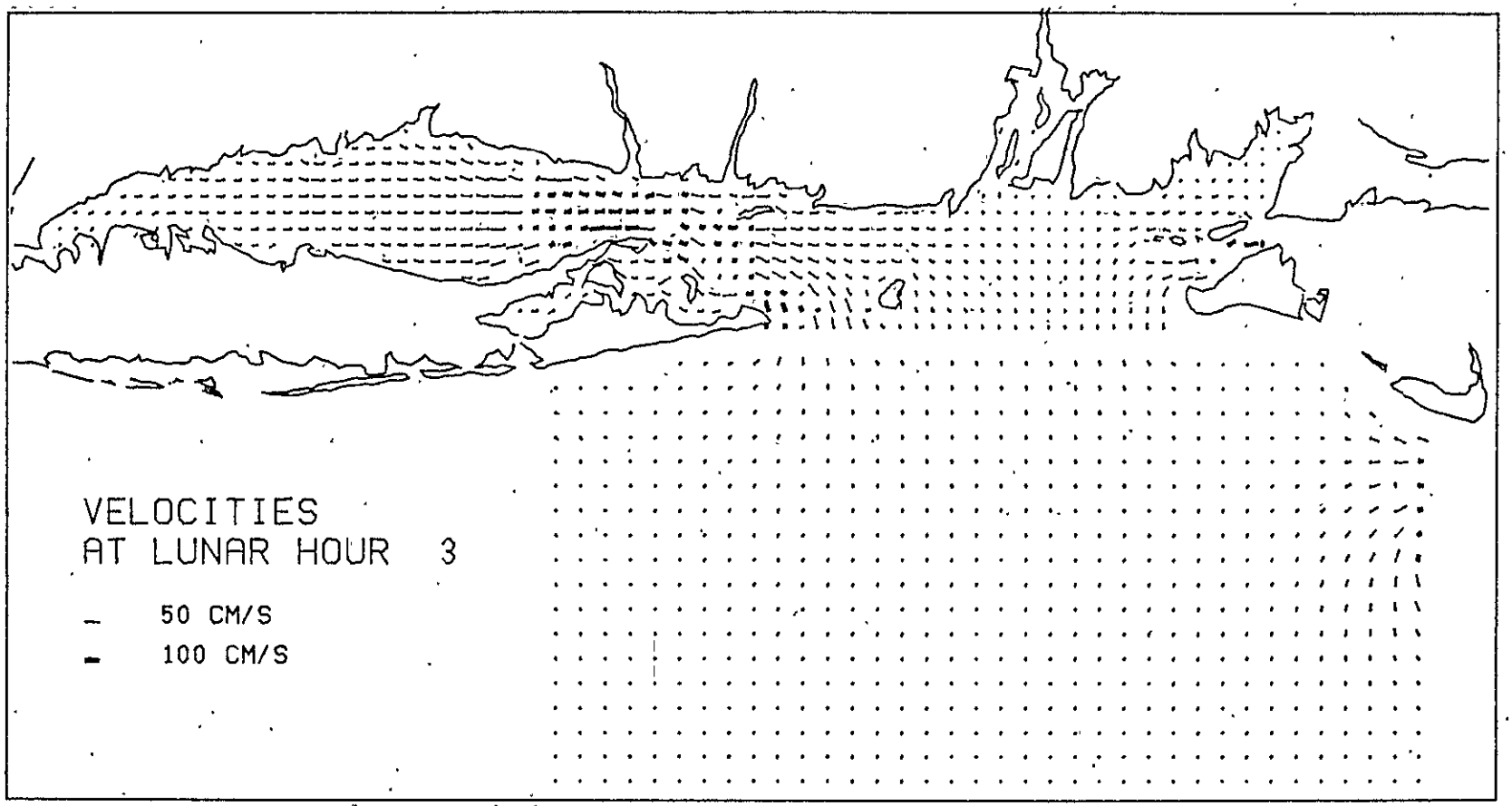

IV.10 COMPUTED VELOCITY VECTORS AT LUNAR HOUR 3.

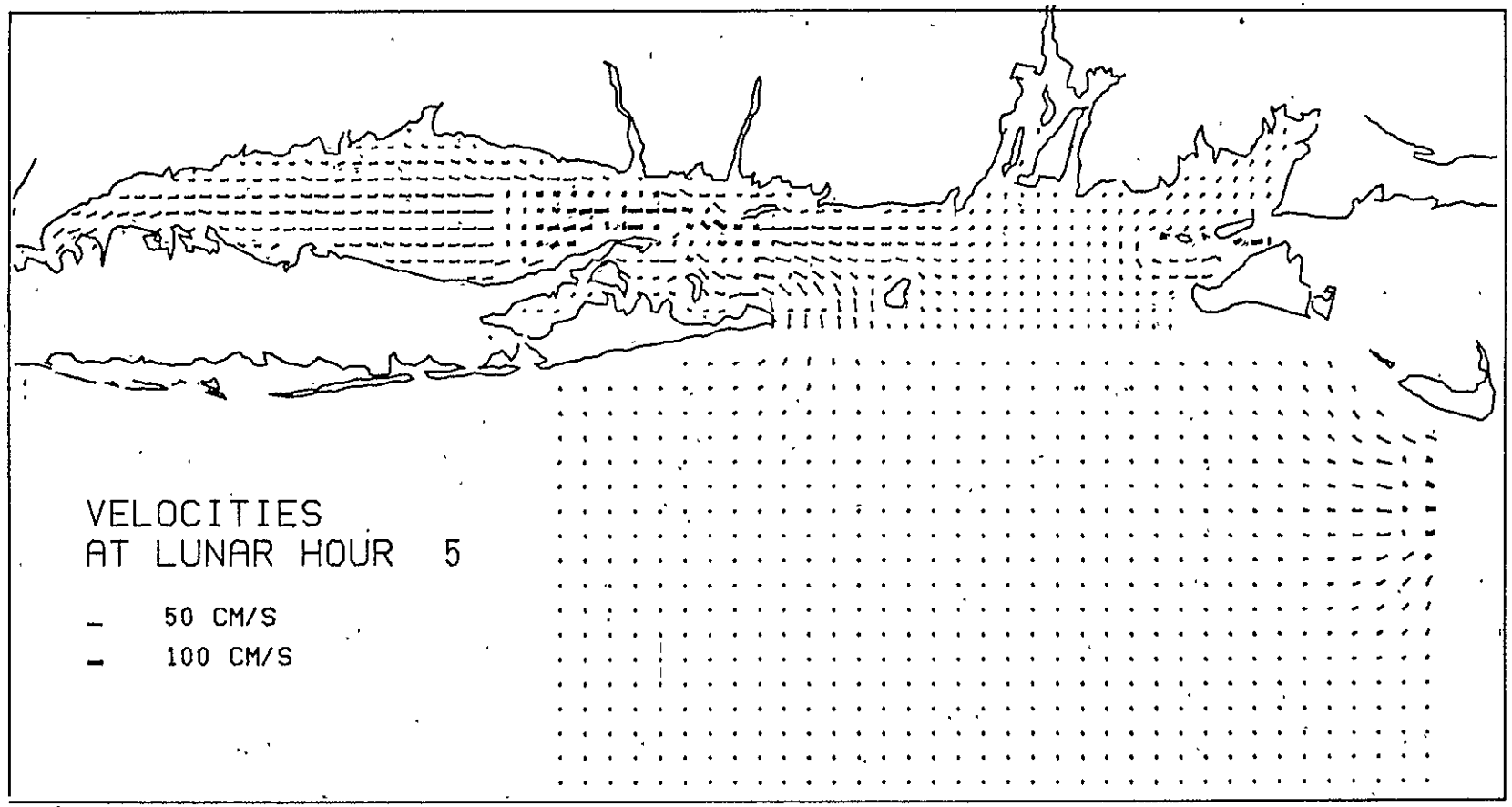

IV.11 COMPUTED VELOCITY VECTORS AT LUNAR HOUR 5.

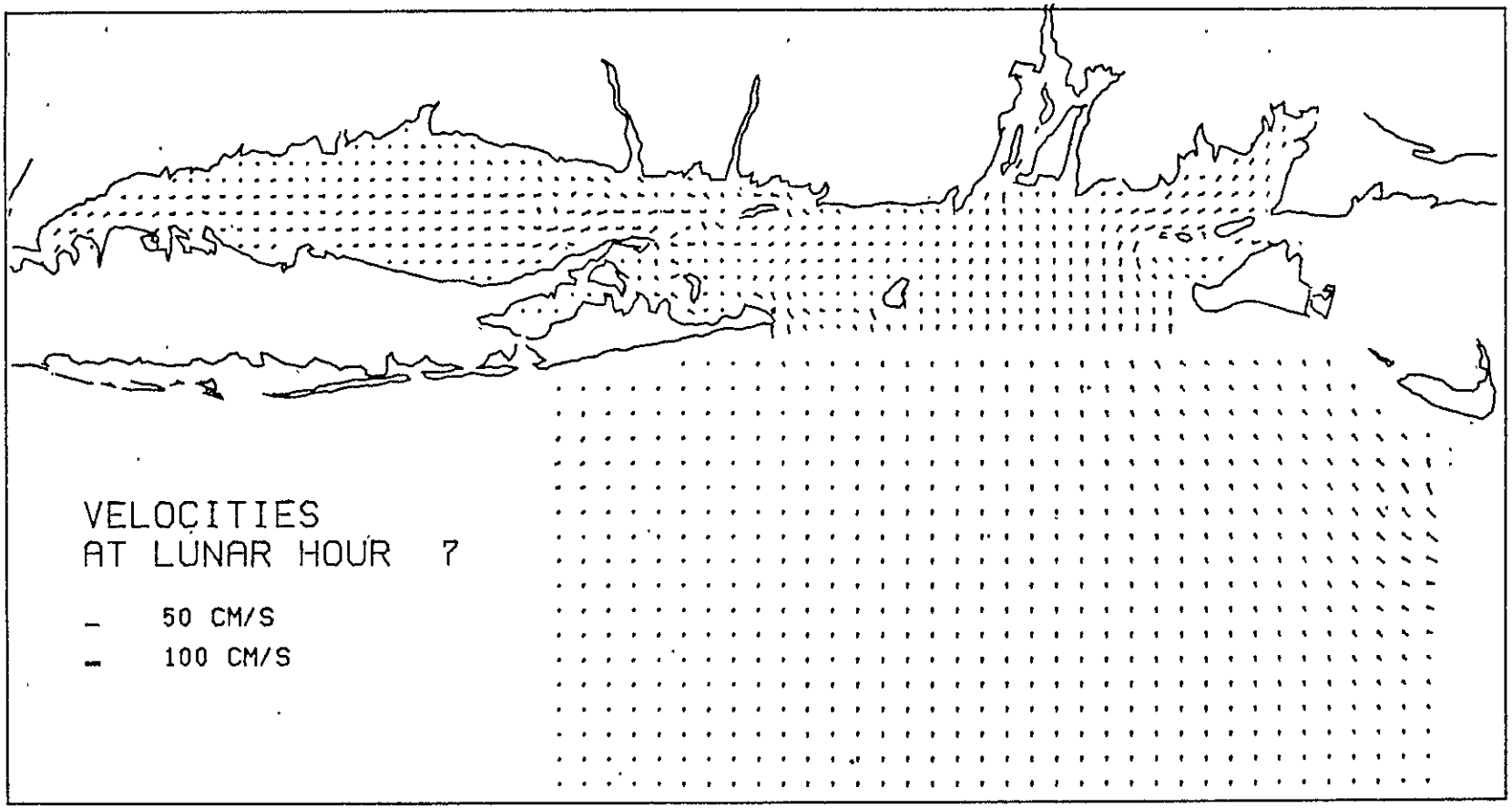

IV.12 COMPUTED VELOCITY VECTORS AT LUNAR HOUR 7.

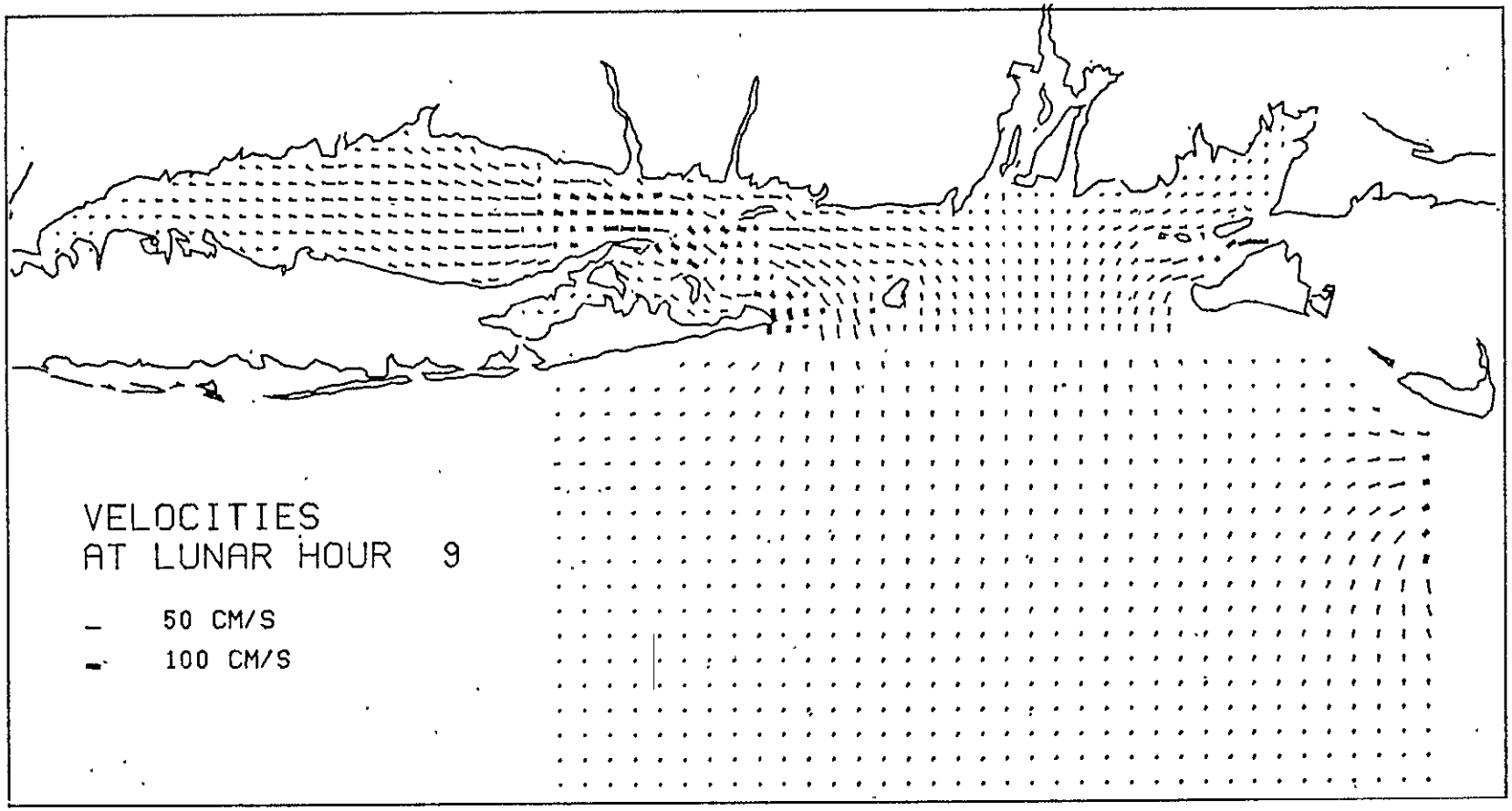

IV.13 COMPUTED VELOCITY VECTORS AT LUNAR HOUR 9.

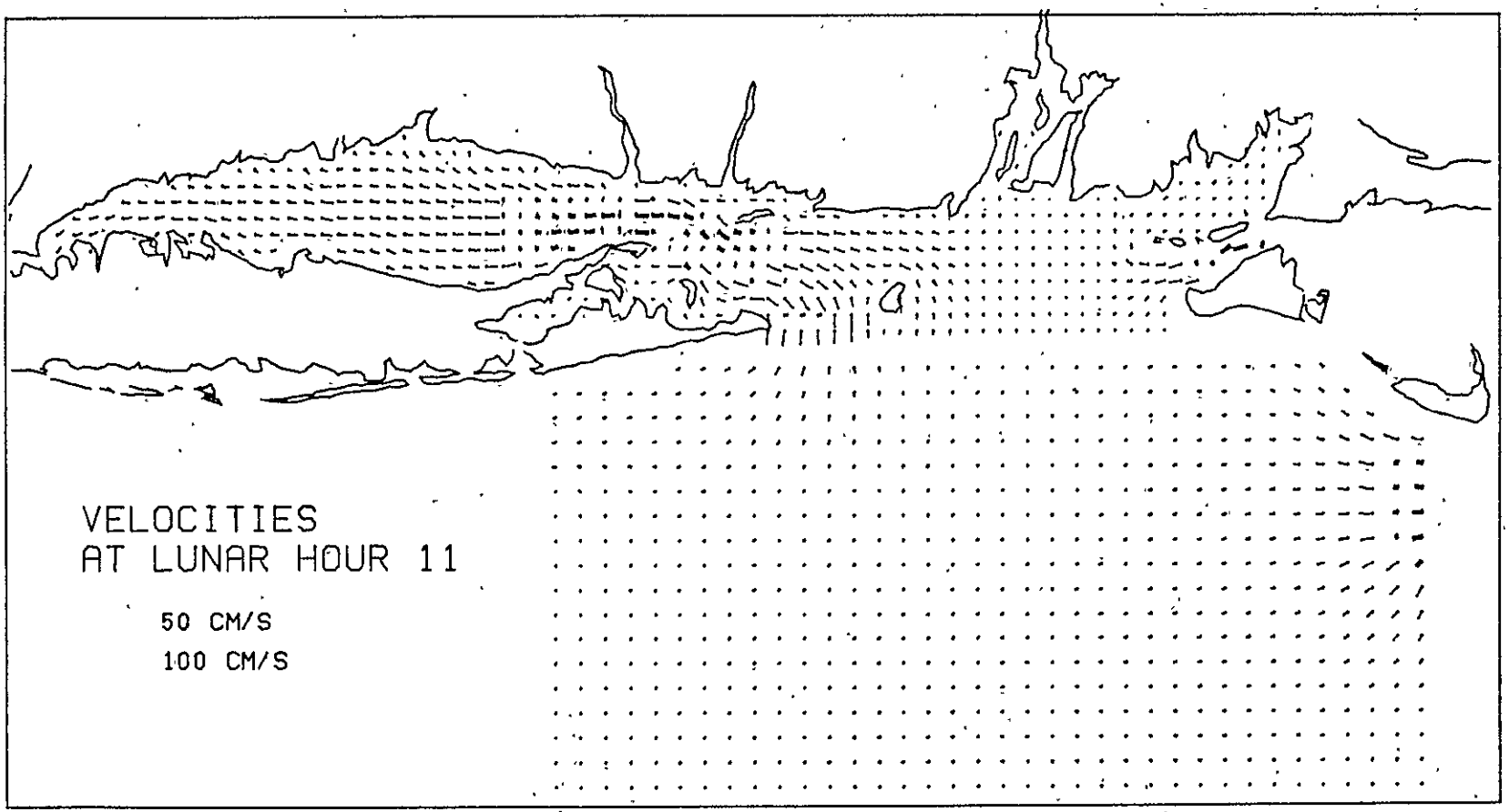

IV.14 COMPUTED VELOCITY VECTORS AT LUNAR HOUR 11.